

Characterization of Tobacco ringspot virus and its nematode vector, *Xiphinema rivesi*, infecting Highbush Blueberry in Washington State

Arunabha Mitra,^{1,2} Sridhar Jarugula,¹ Segun A. Akinbade,³ Zafar Handoo,⁴ Mihail Kantor,⁴ Joseph D. Mowery,^{5,@} and Rayapati A. Naidu^{1,*}

¹Department of Plant Pathology, Washington State University, Irrigated Agriculture Research and Extension Center, 24106 N Bunn Rd, Prosser, WA 99350, USA

²Current Address: Department of Microbiology and Plant Pathology, University of California, Riverside, CA 92521, USA

³Washington State Department of Agriculture, Prosser, WA 99350, USA

⁴Mycology and Nematology Genetic Diversity and Biology Laboratory, United States Department of Agriculture (USDA), Agricultural Research Service (ARS), Northeast Area, Beltsville, MD 20705, USA

⁵Electron and Confocal Microscopy, USDA, ARS, Northeast Area, Beltsville, MD 20705, USA

@Current address: ZEISS Research Microscopy Solutions, Carl Zeiss Microscopy, LLC, One North Broadway, White Plains, NY 10601, USA

*Corresponding author: naidu.rayapati@wsu.edu

Abstract

Highbush blueberry (*Vaccinium corymbosum* L.) plants showing stunting and severe defoliation were observed in an organic blueberry farm in eastern Washington State. Initially, leaves of affected blueberry plants showed crinkling and mottling, chlorotic spots and red-colored rings with chlorotic centers. Subsequently, infected plants showed severe defoliation with overall decline within a few years. Symptomatic blueberry plants produced small berries of uneven size and poor ripening compared to berries of uniform ripening produced by healthy plants. Berries from symptomatic plants showed significant reduction in total soluble solids, juice pH and total anthocyanins, and increased titratable acidity compared to berries from healthy plants. High-throughput sequencing of total RNA extracted from symptomatic leaves revealed the presence of Tobacco ringspot virus (genus *Nepovirus*, family *Secoviridae*). The complete genome sequence of the RNA1 and RNA2 segments was determined, respectively, to be 7,512 and 3,925 nucleotides, excluding the 3'-terminal poly(A) tail. In RT-PCR assays, a portion of the Pro-Pol domain of RNA1 and the Coat Protein (CP) gene encoded by RNA2 were amplified only from symptomatic blueberry plants. In phylogenetic analyses, the TRSV isolate from blueberry clustered with viral species in *Nepovirus* sub-group A based on the conserved CG-GDD motif of the Pro-Pol domain of RNA1 and the conserved sequence in the CP of RNA2. The detection of TRSV in adult female dagger nematodes extracted from soil samples collected near symptomatic blueberry plants and in-field transmission assays using cucumber bait plants implicated nematode transmission of TRSV. The dagger nematode was identified as *Xiphinema rivesi* Dalmasso, 1969 using a combination of morphological and morphometric data and phylogenetic analysis of nucleotide sequences specific to

D2-D3 expansion domains of the 28S rRNA gene and the internal transcribed spacer region of nematode species within the genus *Xiphinema*.

Keywords: Tobacco ringspot virus, Nepovirus, High-throughput sequencing, *Vaccinium corymbosum*, *Xiphinema rivesi*

Introduction

Tobacco ringspot virus (TRSV), type member of the genus *Nepovirus* in the family *Secoviridae* (Sanfaçon et al. 2009), was first reported in 1927 from *Nicotiana tabacum* (Fromme et al. 1927). TRSV belongs to sub-group A in the genus *Nepovirus* with RNA1 and RNA2 genome segments of sizes ~7.5 kb and ~3.9 kb, respectively (Chandrasekar and Johnson 1998; Digiaro et al. 2007; Zhao et al. 2015). TRSV particles are also known to be routinely associated with low molecular weight RNA species packaged in self-contained particles that depend on the presence of TRSV for their own replication. These additional encapsidated RNA molecules associated with TRSV infection are called satellite TRSV particles (SL-TRSV). The SL-TRSV capsid is derived from the TRSV genome and each SL-TRSV particle contains 14-26 uniform molecules of biologically active RNA (Buzayan et al. 1986; Rezaian and Jackson 1981; Schneider 1971; Schneider and White 1976).

TRSV has a very broad host range including herbaceous and woody plants (Price 1940; Stace-Smith 1985; Zhao et al. 2015). The virus is known to cause economically significant diseases in tobacco, soybean, tomato, cucumber, blueberry, and grapevine worldwide (Fuchs et al. 2010; Gilmer et al. 1970; Rowhani et al. 2017; Šneideris et al.

2012, Zhao et al. 2015). TRSV is readily transmissible by manual inoculation, through seed, and by soil-borne ectoparasitic nematodes belonging to the *Xiphinema americanum* species complex (dagger nematodes) in a persistent manner (McGuire et al. 1970; Mink 1993; Owusu et al. 1968; Wang et al. 2002; Yang and Hamilton 1974).

With over 180 million pounds of production in 2022, Washington State became the national leader in blueberry production, with more organic blueberries produced in the state than in all other 49 states combined (Courtney and Mullinax 2020; DeVetter et al. 2015; NASS, 2022). Although blueberries were traditionally cultivated in Western Washington, recent years have witnessed an increased acreage of blueberries in Eastern Washington, especially organic blueberries (DeVetter et al. 2015). Between 2015 and 2019, highbush blueberry (*Vaccinium corymbosum* L.) plants of cultivars (cvs.) Draper and Top Shelf showing severe defoliation and stunting symptoms were observed in an organic farm in eastern Washington State. In initial studies, samples from symptomatic plants tested negative for Blueberry scorch (BIScV) and Blueberry shock (BIShV) viruses, two economically important viruses widely distributed in blueberry-growing regions (Martin and Tzanetakis 2018). In serological assays, symptomatic leaves from infected blueberry plants tested positive only for TRSV (Mitra et al. 2021).

Since this is the first report of TRSV infecting highbush blueberry in the Pacific Northwest (Martin and Tzanetakis 2018; Mitra et al. 2021), this study was undertaken to molecularly characterize TRSV, examine impacts of the virus on fruit quality attributes, conduct field studies to demonstrate soil-transmission of TRSV using in-field cucumber bait plant assays and confirm the dagger nematode, *Xiphinema rivesi* Dalmasso, 1969, as a vector of TRSV.

Materials and Methods

Plant samples

A four-acre organic highbush blueberry (*V. corymbosum* L.) farm located in eastern Washington State (name and location of the field are withheld due to confidentiality) was used in this study. This farm was planted in Spring 2015 with five cultivars, namely, Duke, Cargo, Last Call, Draper, and Top Shelf. Blueberry plants were grown under standard cultivation practices (raised beds of 12-16 inches, acidic soil pH 6.0-6.3, with a weed barrier mat). Virus-like symptoms were observed only in cvs. Draper and Top Shelf. Samples were collected randomly from different parts of the canopy from both symptomatic and asymptomatic plants to account for potential uneven virus distribution in infected plants. In previous studies, only TRSV was detected in symptomatic plants but not in non-symptomatic plants (Mitra et al. 2021).

Detection of TRSV by RT-PCR

Leaf samples collected from symptomatic and asymptomatic blueberry plants were extracted using the protocol described earlier (Adiputra et al. 2018; Alabi et al. 2008). Sample extracts were denatured and subsequently used in single tube-one step RT-PCR assay for simultaneous detection of RNA1 and RNA2 genome segments of TRSV using the protocol optimized for the detection of TRSV in grapevines (unpublished data). Three sets of primers were used in RT-PCR assays (Table 1, Mitra et al. 2021). One pair of primers will amplify a ~350 bp fragment of the Helicase (Hel) region (between nt. 3,630

and nt. 4,001) encoded by the TRSV RNA1 segment (MW495243) and the second pair of primers amplify a ~620 bp fragment of the CP region (between nt. 2,340 and nt. 2,989) encoded by the TRSV RNA2 segment (MW495244). The third primer pair was used to amplify a ~181 bp fragment of the mitochondrial NADH dehydrogenase subunit 5 (*nad5*) gene from blueberry (PV173276) as a host-derived mRNA internal positive amplification control (Adiputra et al. 2018; Gutha et al. 2010; Menzel et al. 2002).

The RT-PCR assay was performed in a total reaction volume of 25 μ l containing 1X concentration of the reaction buffer (Roche Diagnostics, IN, USA), 10 mM of each dNTP, 1.25 U of Taq DNA polymerase (Roche Diagnostics, IN, USA), 0.12 μ M of each primer, 5 mM dithiothreitol (DTT), 4 U RNaseOUT™ (ThermoFisher Scientific, MA, USA), and 7 U of SuperScript™ IV reverse transcriptase (ThermoFisher Scientific, MA, USA). The RT-PCR assay was performed with an initial reverse transcription step at 52°C for 30 min, followed by denaturation at 94°C for 2 min, and then 35 consecutive PCR cycles with each cycle consisting of a denaturation step at 94°C for 30 sec, primer annealing step at 56°C for 30 sec, and an extension step at 72°C for 30 sec with a final extension step performed at 72°C for 5 min. RT-PCR assays were carried out in the ProFlex™ PCR system (Applied Biosystems, CA, USA). Five μ l of the RT-PCR product was resolved on 1.0% agarose gel pre-stained with ethidium bromide (0.5 μ g/ml) and the DNA bands visualized in a UV transilluminator (Bio-Rad Molecular Imager®, Bio-Rad Laboratories, Inc., CA, USA). Appropriate positive and negative controls were used in each RT-PCR assay for validation of assay results. RT-PCR amplicons of expected size were cloned, sequenced by Sanger sequencing, and the derived sequences were subjected to

BLASTn search to examine their alignment with TRSV sequences deposited in GenBank (<https://www.ncbi.nlm.nih.gov/geo/query/blast.html>).

Total RNA extraction and high-throughput sequencing

Total RNA was extracted from ~100 mg of leaf tissue collected from a symptomatic blueberry plant using the Spectrum™ Plant Total RNA Kit (Sigma-Aldrich, Inc., MO, USA), according to the manufacturer's instructions. The concentration and quality of total RNA was estimated using the NanoDrop™ 2000 Spectrophotometer (ThermoFisher Scientific, MA, USA). RNA Integrity Number (RIN) of total RNA was measured on the 2100 Bioanalyzer Instrument (Agilent Technologies, Inc., CA, USA). Aliquots of ~20µL total RNA with >7.0 RIN were shipped to the Huntsman Cancer Institute (HCI) at the University of Utah, USA, for high-throughput sequencing (HTS) on the Illumina® NovaSeq™ platform. cDNA library preparation was performed at HCI using the Illumina® TruSeq® Stranded Total RNA Library Prep Plant kit (Illumina®, Inc., CA, USA) and subjected to HTS using the NovaSeq 6000 Sequencing System (Illumina®, Inc., CA, USA).

The 150 nucleotide (nt) paired-end raw reads were imported into CLC Genomics Workbench v12.0 (Qiagen Digital Insights, Qiagen®, MD, USA) and subjected to trimming to remove adapter sequences and low-quality reads. Reference-guided mapping of the 150 nt paired-end, quality-filtered reads was conducted against a NCBI-sourced virus and viroid genome reference database (<https://ftp.ncbi.nlm.nih.gov/refseq/release/viral/>) filtered to only include virus accessions having genomes below 20 kb in size, with a stringency level of 0.5/0.8 (length/similarity). *De novo* assembly of the paired-end reads

was performed with word size 23, bubble size 50, and minimum contig length 200 nt. During the *de novo* assembly operation, the RNAseq reads were mapped back to the contig sequences with a 0.5/0.8 length/similarity stringency. Finally, contigs were screened based on length (base pair, bp), number of reads corresponding to each contig, and read coverage. Screened contigs were subjected to nucleotide BLAST (BLASTn) search on NCBI to examine whether they aligned with plant virus sequences deposited in GenBank (<https://www.ncbi.nlm.nih.gov/geo/query/blast.html>).

Sequence analysis of RNA1 and RNA2 genome segments of TRSV

The *de novo* contigs from the HTS reads were used to generate complete RNA1 and RNA2 sequences of the TRSV isolate genome. In the case of the RNA2 segment, a near-complete segment sequence was generated from *de novo* contigs. In contrast, *de novo* assembly of RNA1-specific HTS reads produced two contigs with four gaps that were subsequently completed by Sanger sequencing. For this purpose, primers (Table S1) were designed based on the sequence of *de novo* contigs corresponding to the RNA1 segment. The total RNA preparation used for HTS was used for cDNA synthesis using the SuperScript™ IV First Strand Synthesis System (Thermo Fisher Scientific, MA, USA) with 50 µM random hexamers (New England Biolab, MA, USA) following the manufacturer's instructions. The cDNA was used as a template in PCR for amplification of gaps in the RNA1 segment. PCR assays were carried out in a 25 µl volume consisting of 1X concentration of reaction buffer (Roche Diagnostics, IN, USA), 10 mM of each dNTP, 1.25 U of Taq DNA polymerase (Roche Diagnostics, IN, USA), and 1 µM each of the forward and reverse primers (Table S1). The PCR run parameters consisted of an

initial denaturation at 94°C for 3 min, followed by 35 consecutive PCR cycles with each cycle having a denaturation step at 94°C for 10 sec, an annealing step at 60°C for 15 sec, and an extension step at 72°C for 1 min, and a final extension step at 72°C for 3 min. Amplicons of the expected size were cloned into the pCR™2.1-TOPO™ vector (ThermoFisher Scientific, MA, USA) and recombinant clones transformed into One Shot™ TOP10 chemically competent *Escherichia coli* (ThermoFisher Scientific, MA, USA). Three independent clones per amplicon were subjected to Sanger sequencing in both orientations (GenScript, NJ, USA). The derived sequences, together with the *de novo* assembled contigs, were used to generate the near-complete nucleotide sequences of RNA1 and RNA2 genome segments of the TRSV isolate.

The 5'-end sequence of TRSV RNA1 and RNA2 segments was verified by rapid amplification of cDNA ends (RACE) using a commercial 5'-RACE system (Version 2.0, ThermoFisher Scientific, MA, USA), following the manufacturer's protocol. Primers used for the 5'-RACE are listed in Table S1. First-strand cDNA was synthesized from total RNA preparations using an RNA1- or RNA2-specific reverse primer and purified using the S.N.A.P.™ Gel Purification Kit (ThermoFisher Scientific, MA, USA). A homopolymeric dC tail was ligated to the 3'-end of the purified cDNA using terminal deoxynucleotidyl transferase (TdT) supplied with the 5'-RACE kit. This dC-tailed cDNA was used as the PCR template with the abridged anchor primer (AAP, supplied with the 5'-RACE kit) and segment-specific reverse primer (GSP1, Table S1). The diluted (1:100 v/v) PCR product used was as template in nested PCR using abridged universal amplification primer (AUAP, supplied with the 5'-RACE kit) and a second segment-specific reverse primer (GSP2, Table S1). PCR amplicons of the expected sizes were cloned and sequenced as

described earlier. The derived sequences were used to determine the 5'-end sequence for both TRSV RNA1 and RNA2 segments.

To verify the 3'-end sequence of TRSV RNA1 and RNA2, three nested forward primers (GSP4, GSP5, and GSP6, Table S1) were designed proximal to the 3'-end based on the RNA1 and RNA2 *de novo* contig sequences. Individual RT-PCR reactions were set up with each forward primer and a common poly(T) reverse primer which would anneal to the 3'-end poly(A) tail of the virus genomic RNA. Two μl aliquots of total RNA preparations were used as template for the RT-PCR. The RT-PCR reaction volume was 25 μl total, containing 1X concentration of reaction buffer (Roche Diagnostics, IN, USA) consisting of 1 mM Mg^{2+} , 10 mM of each dNTP, 1.25 U of Taq DNA polymerase (Roche Diagnostics, IN, USA), 1 μM each of the primers, 5 mM DTT, 4 U RNaseOUT™ (ThermoFisher Scientific, MA, USA), and 7 U of SuperScript™ IV reverse transcriptase (ThermoFisher Scientific, MA, USA). The RT-PCR cycle consisted of initial incubation at 52°C for 30 min and then 94°C for 2 min, followed by 35 cycles of denaturation at 94°C for 20 sec, annealing at 55°C for 20 sec, and extension at 72°C for 1 min, followed by a final extension at 72°C for 7 min. Amplicons of expected size were cloned, sequenced, and the derived sequences were used to determine the 3'-end sequence for both TRSV RNA1 and RNA2 segments. Translation of the complete nucleotide sequences of both TRSV genome segments was performed using the ExPASy Translate tool (<https://web.expasy.org/translate/>) and molecular weights of the putative polyproteins were determined via the Protein Molecular Weight tool on www.bioinformatics.org (https://www.bioinformatics.org/sms/prot_mw.html).

Phylogenetic analyses of TRSV

Phylogenetic analyses were conducted using polyprotein sequences of TRSV isolate (WA-AM1) from cv. Draper and representative isolates from GenBank in the genus *Nepovirus*. The Pro-Pol and CP regions of the RNA1 and RNA2 genome segments, respectively, were subjected to multiple sequence alignments via MUSCLE (Edgar 2004) on MEGAX (Kumar et al. 2018), followed by phylogenetic tree construction by the Maximum-likelihood (ML) algorithm. For both amino acid sequence alignments, the best ML model predicted by MEGAX was the Le-Gascuel (LG) model (Le and Gascuel 2008). Evolutionary rate differences among the sites were modeled using a discrete Gamma distribution (+G, 5 categories). Phylograms with the highest log likelihood from 1,000 bootstrap replications were taken into consideration. Bootstrap support values more than 70% were displayed at the branch nodes and branches showing less than 70% bootstrap support collapsed.

Impact of TRSV on fruit quality

At the time of commercial harvest, blueberries were harvested from five symptomatic plants (cv. Draper) tested positive for TRSV and five plants without symptoms and tested negative for the virus. Blueberries harvested from TRSV-positive and TRSV-negative plants were pooled separately and divided into five replicates with 25 berries for each replicate for biochemical analysis. After taking weights (g), berries were homogenized using an IKA[®] A 11 basic Analytical Mill (IKA Works, Inc., NC, USA). The homogenate was clarified by centrifugation at 3,500 rpm for 5 min in an Eppendorf[®] Centrifuge 5804 R (Eppendorf, Germany) and the supernatant (berry juice) was used for

measuring total soluble solids (TSS, measured as °Brix), juice pH, titratable acidity (TA), and total anthocyanins following the methodology described by Alabi et al. (2016). Juice pH was measured using a Hanna® HI5222K two-channel benchtop pH meter (Hanna Instruments, RI, USA). A PAL-1 digital pocket refractometer (Atago Inc., WA, USA) was used to estimate TSS as °Brix (1 °Brix = 1 g of sucrose in 100 g of solution). Berry juice TA was measured using 5 ml of juice per replicate. The volume of NaOH used for juice acid neutralization was recorded for calculating TA as shown below:

$$\text{TA (grams of Tartaric acid/100 milliliters of juice)} = \frac{\text{Volume of 0.1N NaOH used (ml)}}{\text{Volume of juice used (ml)}} \times 7.5$$

Total anthocyanins from berry homogenates were estimated according to the method described earlier (Illand et al. 2000). Berry weight (g) and OD₅₂₀ value were used to calculate the total anthocyanins, according to the following formula:

$$\text{Total anthocyanins} = \left(\frac{\text{OD}_{520}}{500} \right) \times 11 \times 0.095 \times \text{berry weight (g)} \times \left(\frac{1000}{\text{berry weight (g)}} \right)$$

Statistical analysis of the fruit quality data was conducted via a two-tailed t-test with a 0.05 *p*-value threshold for significance.

Identification of dagger nematodes

Soil samples were collected 6-12 inches below the soil surface close to the root zone of symptomatic, TRSV-positive blueberry plants (cv. Draper) using a soil probe (Wojtowicz et al. 1982). Six soil cores (2.5 cm x 20 cm deep) were collected from each sample area and pooled into a plastic bag. Soil samples from six locations were collected for this study. The soil sample from each bag was mixed thoroughly and approximately

250 g of soil sample from each bag was processed by decanting and sieving followed by sucrose centrifugal floatation to extract nematodes from the soil (Jenkins 1964).

The nematode suspensions were examined under a Leica[®] M80 stereo microscope (Leica Microsystems Inc., IL, USA) to identify dagger nematodes (*Xiphinema* spp.) based on visual observations. Candidate dagger nematodes were individually handpicked onto a drop of water on a glass slide using a needle probe and examined further under the microscope for identification based on morphological characteristics (Akinbade et al. 2014). Further validation of nematode identity was conducted by molecular analysis targeting nematode nuclear ribosomal DNA (rDNA). For this purpose, individual and pooled (n = 2 to 5) adult nematodes were homogenized with a micro-pestle in 20 µl of nematode lysis buffer in a 1.7 ml Eppendorf[®] (Eppendorf, Germany) microcentrifuge tube, denatured, and used as a template for PCR amplification of two separate ribosomal RNA (rRNA)-coding regions in nuclear DNA, as described earlier (Skantar et al. 2012, Thomas et al. 1997; Williams et al. 1992; Zasada et al. 2014).

One set of primers (D2A and D3B, Skantar et al. 2012) was used to amplify a ~840 bp DNA fragment specific to the D2-D3 expansion segment of the 28S large ribosomal subunit (LSU). A second set of primers (TW81 and AB28, Skantar et al. 2012) was used to amplify a ~1,360 bp DNA fragment specific to the internal transcribed spacer (ITS) rDNA-coding region comprising ITS1-, 5.8S rRNA-, and ITS2-coding regions. The PCR run parameters followed were as described by Skantar et al. (2012) and amplicons of the expected size were cloned and sequenced as described in earlier sections. The derived nucleotide sequences were subjected to a BLAST (BLASTn) search on NCBI (<https://www.ncbi.nlm.nih.gov/geo/query/blast.html>) to confirm their alignment with

Xiphinema spp. sequences from the *X. americanum* group in GenBank. In addition, pairwise nucleotide identity matrices were generated for the D2-D3 expansion segment and ITS rRNA-coding sequences with corresponding sequences of representative *X. americanum* isolates from GenBank on MEGAX (Kumar et al. 2018). In the case of the D2-D3 expansion segment, a total of 27 sequences were included in the analysis and aligned via MUSCLE (Edgar 2004) with 712 positions in the alignment. In the case of the ITS rRNA-coding region, a total of 13 sequences were included in the analysis. The sequences were aligned via MUSCLE and there were 859 positions in the alignment.

To investigate the evolutionary relationship of the dagger nematodes identified in this study with other *X. americanum*-group members, an ML phylogenetic tree was constructed using the nucleotide sequence corresponding to the D2-D3 expansion segment obtained from this study (PQ452334) and corresponding sequences from representative species in the *X. americanum*-group obtained from GenBank. This phylogram was constructed in MEGAX (Kumar et al. 2018) using the General Time Reversible (GTR, Nei and Kumar 2000) model with a discrete Gamma distribution to model evolutionary rate differences among sites (5 categories (+G, parameter = 0.9338)). The rate variation model allowed for some sites to be evolutionarily invariable ([+I], 30.18% sites). This GTR+G+I was the best suited ML model for our selected sequence set, as determined by MEGAX. The final phylogram generated from 1,000 bootstrap replications was taken into consideration.

Individual nematode samples were shipped to the USDA Mycology and Nematology Genetic Diversity and Biology Laboratory in Beltsville, MD, USA, for Low-Temperature Scanning Electron Microscope (LT-SEM) imaging. Morphometric

measurements were taken for individual nematodes for identification of nematodes in the family *Longidoridae* (de Man 1877; Handoo et al. 2015; Farahnaz et al. 2020; Jairajpuri and Ahmad 1992). Nematodes were fixed in 3% formaldehyde and processed to glycerin by the formalin glycerin method (Golden 1990; Hooper 1970). Photomicrographs of the specimens were made with a Nikon Eclipse Ni compound microscope using a Nikon DS-Ri2 camera (Nikon Inc., IL, USA). Morphometric details of 20 adult nematode specimens from soil samples were recorded using taxonomic keys and published literature to identify the nematode species (Handoo et al. 2015; Lamberti and Carone 1991; Loof and Luc 1993; Wojtowicz et al. 1982). Measurements were made with an ocular micrometer on a Leica WILD MPS 48, Leitz DMRB compound microscope (Leica Microsystems Inc., IL, USA). All measurements were taken in micrometers (μm) unless otherwise stated. For the LT-SEM imaging, nematode specimens were prepared and observed using the techniques described in Carta et al. (2020) and Kantor et al. (2020).

Detection of TRSV in dagger nematodes

Total RNA was extracted from adult female dagger nematodes isolated from soil samples using the RNeasy® Mini kit (Qiagen®, MD, USA). Prior to extraction, individual and pooled (count = 2 to 4) samples of isolated nematode adults were taken in RLT buffer (supplied with the kit) containing 50 mM DTT and homogenized (Demangeat et al. 2004), followed by total RNA isolation according to the manufacturer's protocols. Synthesis of cDNA was carried out using the SuperScript™ IV First Strand Synthesis System (Thermo Fisher Scientific, MA, USA) with 50 μM random hexamers (New England Biolab, MA, USA). A 2 μl aliquot of cDNA was used as a template in PCR assays for the detection of

TRSV using primers and assay conditions described earlier. A single amplicon corresponding to the TRSV RNA1 segment was cloned and sequenced as described earlier. The derived sequences were compared with TRSV sequences available in GenBank for confirmation.

Cucumber bait plant bioassay for TRSV transmission

An in-field cucumber bait plant assay was conducted to examine the spread of TRSV by the soil-borne dagger nematodes (Širca et al. 2007). In May 2019, 10 to 12 cucumber seedlings (*Cucumis sativus*, cv. Boston Pickling) were planted in the blueberry field in two locations where symptomatic plants (cv. Draper) had been present (five to six seedlings for each location). These cucumber seedlings were maintained in the field until October 2019. Between May and October, cucumber plants were monitored for virus-like symptoms and leaf samples collected in July (two months post-planting) and September (four months post-planting) were tested for TRSV by RT-PCR with primers specific to a portion of the CP or Hel (Table 1). RT-PCR assays were carried out as described above. Amplicons of the expected size from TRSV-positive cucumber samples were subjected to cloning and Sanger sequencing as described earlier. The derived sequences were compared with TRSV-specific sequences available in GenBank for confirmation. This in-field bioassay was repeated in 2020, with ten cucumber seedlings (*C. sativus*, cv. Boston Pickling) planted at the same in-field locations as in 2019. The cucumber seedlings were planted in June 2020 and tested by RT-PCR in August (two months post-planting) and October (four months post-planting) for the presence of TRSV by RT-PCR as described above. For additional confirmation of TRSV in cucumber bait plants, total RNA was

isolated from two symptomatic cucumber plants in 2019 and three symptomatic plants in 2020 and subjected to HTS on the Illumina® NovaSeq™ platform. The *de novo* contigs from the HTS reads were subsequently used to generate near-complete RNA1 and RNA2 sequences as described above.

Results

Symptoms in TRSV- infected highbush blueberry plants

The symptomatic blueberry plants of cvs. Draper and Top Shelf showed poor growth and a wide range of foliar symptoms that included severe defoliation, crinkling, mottling, chlorotic spots, and red-colored rings with chlorotic centers on leaves (Figure 1). Symptomatic plants had fewer leaves than healthy plants with small clusters and uneven size and ripening of berries. Although severe symptoms were observed throughout the canopy of several blueberry plants, a few plants showed symptoms only in a few branches with the other branches showing normal growth and healthy-appearing canopy. As the season advanced, plants with severe symptoms produced a flush of new leaves indicating possible recovery. However, symptomatic plants showed gradual declining leading to death within a few years after planting.

Detection of TRSV RNA1 and RNA2

Extracts of leaves collected from symptomatic and asymptomatic blueberry were tested by RT-PCR using primers specific to a region of the Hel gene encoded by RNA1

and the CP gene encoded by RNA2 (Table 1). Leaf samples from eight symptomatic and seven asymptomatic blueberry plants (10 from cv. Draper and seven from cv. Top Shelf) were tested for the presence of TRSV. As shown in Figure 2, an approximately 372 bp fragment specific to Hel gene and an approximately 647 bp fragment specific to the CP were amplified only from symptomatic samples suggesting correlation between symptoms and the presence of TRSV. The amplification of an approximately 180 bp fragment of the *nad5* gene in all samples, irrespective of whether blueberry samples tested positive or negative for TRSV, enabled reliable interpretation of RT-PCR assay results. Sanger sequencing of amplicons specific to TRSV-RNA1 and -RNA2 (MW514264 to MW514298) showed 97% and 98% identities at the nt level with corresponding sequences of TRSV isolates IA-1-2017 (MT563079) and SK (KJ556849), respectively, reported from Iowa and South Korea producing bud blight symptoms in soybean (*Glycine max* L. Merr.). These results confirmed serological data reported earlier (Mitra et al. 2021) for the presence of TRSV in symptomatic blueberry plants.

Impacts on fruit quality in TRSV-infected highbush blueberry plants

To examine the effects of TRSV on fruit quality, blueberries were harvested from symptomatic plants tested positive for TRSV and asymptomatic plants tested negative for TRSV in RT-PCR assays from cv. Draper. As shown in Table 2, berries from symptomatic, TRSV-positive plants had significantly ($p < 0.05$) reduced fruit weight, sugar content, juice pH, and total anthocyanins compared to berries from asymptomatic, TRSV-negative plants. In contrast, TA of berries collected from TRSV-positive plants was nearly two-fold higher than berries from TRSV-negative plants. Based on these results, it can be

concluded that TRSV negatively impacts blueberry fruit yield and quality attributes, such as sugars and anthocyanins that are hallmarks of fruit quality.

TRSV genome characterization and phylogenetic analyses

Since many viruses can infect blueberries, either as single or co-infections, causing a wide range of symptoms ranging from asymptomatic to plant death (Martin et al. 2012, Martin and Tzanetakis 2018), high quality RNA from symptomatic leaf samples was subjected to HTS to examine the virome associated with symptoms observed in blueberry plants. The quality-filtered 150 nt paired-end reads obtained from HTS were subjected to reference-guided mapping and *de novo* assembly (Table 3). In the reference-guided mapping using plant virus and viroid database from GenBank, 78,497 and 25,383 quality-filtered reads mapped, respectively, to RNA1 and RNA2 of TRSV. The quality reads were not mapped to other currently known viruses infecting blueberries. *De novo* assembly of the TRSV-specific reads yielded three contigs, two corresponding to RNA1 and one corresponding to RNA2. The RNA1-specific contigs, measuring 2,778 bp (average coverage = 11,031.7) and 3,589 bp (average coverage = 11,882) had highest nucleotide sequence identity with TRSV isolate from South Korea (KJ556849) and the RNA2-specific contig, measuring 3,615 bp (average coverage = 7,072.1), with TRSV isolate from Iowa, USA (MT563079). Since these contigs did not yield complete coverage of RNA1 and RNA2 genome segments, internal gaps in the sequence were filled by Sanger sequencing of amplicons generated by segment-specific primers. The 5'- and 3'-terminal sequences of TRSV RNA1 and RNA2 genome segments were confirmed by Sanger sequencing of RACE products.

The complete sequence of RNA1 and RNA2 genome segments was determined, respectively, to be 7,512 nt (MW495243) and 3,925 nt (MW495244) in size excluding the 3'-terminal poly(A) tail (Figure 3A, Mitra et al. 2021). The RNA1 segment encoded a single polyprotein of 2,303 amino acids (256 kDa) and showed 97.4% identity with RNA1-encoded polyprotein of the South Korean isolate (AIA10370). The RNA2 segment encoded a single polyprotein of 1,100 amino acids (122 kDa) showing 96.5% identity with RNA2-encoded polyprotein of an isolate from California (QJT41630). These values clearly established that TRSV isolate WA-AM1 sequenced in this study is a strain of TRSV, based on the current criteria for demarcation of viruses as distinct species or strains in the family *Secoviridae* (Lefkowitz et al. 2018; Yang et al. 2020). In comparison with previously characterized TRSV isolates and other members of *Nepovirus* sub-group A, putative protease cleavage sites for RNA1- and RNA2-encoded polyproteins were determined for TRSV isolate WA-AM1 (Buckley et al. 1993; Carrier 1999; Fuchs et al. 2017; Yang et al. 2020). The RNA1-encoded polyprotein was predicted to have four cleavage sites, C⁶³⁷/S⁶³⁸, A¹²³⁹/S¹²⁴⁰, G¹²⁶⁹/A¹²⁷⁰, and C¹⁴⁸⁵/S¹⁴⁸⁶. The RNA2-encoded polyprotein was predicted to have two cleavage sites, C²²⁶/A²²⁷ and C⁵⁸⁶/A⁵⁸⁷ (Figure 3A).

In previous studies, phylogenetic analyses of nepoviruses in the *Secoviridae* family have been conducted using the amino acid sequence spanning the conserved CG-GDD motif of the Pro-Pol domain of RNA1 and the conserved sequence in the CP of RNA2 (Maclot et al. 2021; Yang et al. 2020). We used similar approaches to examine pairwise sequence identities and phylogenetic relationships of conserved Pro-Pol and CP regions of the TRSV isolate WA-AM1 polyprotein sequences. In pairwise comparisons, the conserved Pro-Pol region showed 97.8% identity at nucleotide level and 99.1% identity

at the amino acid level, respectively, with TRSV isolates DSMZ PV-0234 (North Carolina, MW961154) and Budblight (California, MT210150). The CP region showed 94.1% identity at the nucleotide level and 98.5% identity at the amino acid level, respectively, with corresponding sequences of TRSV isolates IA-1-2017 (Iowa, MT563079) and IA-2-2017 (Iowa, MT563081). Based on the species demarcation criteria of 80% in the Pro-Pol region or 75% in the CP region established for the family *Secoviridae* (King et al. 2012), the nucleotide and amino acid sequence identity values suggest that the isolate WA-AM1 characterized from symptomatic blueberry plants is a strain of TRSV rather than a distinct *Nepovirus* species. Sequences corresponding to Pro-Pol and CP sequences of representative viral species in *Nepovirus* sub-groups A, B, and C were included in the phylogenetic analyses. As shown in Figure 3B, TRSV isolate WA-AM1 from blueberry clustered with a reference TRSV isolate from California (NC_005907) in phylogenetic tree using Pro-Pol sequences. In the case of CP-based phylogenetic tree (Figure 3C), the WA-AM1 isolate clustered with the same Californian TRSV isolate (NC_005906).

Identification of the dagger nematode

Initially, nematodes collected from sub-surface soil close to symptomatic, TRSV-positive blueberry plants were examined under a light microscope. Based on the morphological characters of adult forms described by Mai and Lyon (1975) and Wojtowicz et al. (1982), isolated nematodes were identified as *Xiphinema* spp. No other nematode types were observed in the soil samples collected from this field. Subsequently, adult female nematode specimens were further examined by morphometry as well as head and tail morphology at the USDA Mycology and Nematology Genetic Diversity and Biology

Laboratory in Beltsville, MD, USA. A summary of the data is presented in Figure S1 and Table 4. The nematodes showed characteristic features consisting of a gradually tapering body forming a close to open 'C' shape, a rounded lip region continuous with the rest of the body, stirrup-shaped amphids, and a conoid tail usually with a small terminal bulge (Handoo et al. 2015). Based on a comparison of morphological and morphometric features of the adult females with previous species descriptions of dagger nematodes (Table 4, Dalmaso 1969; Fadaei et al. 2003; Handoo et al. 2015; Troccoli et al. 2024; Urek et al. 2005; Wojtowicz et al. 1982), nematodes isolated from the blueberry field were identified as *Xiphinema rivesi* Dalmaso, 1969.

The above results were further confirmed by sequence analysis of PCR amplicons corresponding to the 28S large ribosomal subunit (LSU) D2-D3 expansion segment and the internal transcribed spacer (ITS) rRNA-coding regions including ITS1-, 5.8S rRNA-, and ITS2-coding regions of nuclear rDNA. For the D2-D3 expansion segment, PCR amplicons of approximately 840 bp were obtained from nematode samples. Amplicons from three pooled samples (two with four adult and one with five adult females) were cloned and six clones per sample were sequenced by Sanger sequencing. For the ITS rRNA-coding region, PCR amplicons of approximately 1,360 bp were obtained from three pooled nematode samples mentioned above. Amplicons from these pooled samples were cloned and four clones per sample were sequenced by Sanger sequencing.

Pairwise identity matrices were generated by comparing nucleotide sequences of the D2-D3 expansion segment and ITS rRNA-coding region generated in this study with corresponding sequences of several species in the genus *Xiphinema* (Supplementary Tables S2 and S3). Sequences corresponding to the ~840 bp D2-D3 expansion segment

obtained in this study (PQ452334) had 99.4% nucleotide sequence identity with a corresponding sequence of *X. rivesi* from Maryland (KU680968). Sequences corresponding to the ~1,360 bp ITS rRNA-coding region obtained in from this study (PQ452333) had 95% nucleotide sequence identity with a corresponding sequence of *X. rivesi* from Italy (FR878063). An ML phylogenetic tree was constructed using nucleotide sequences corresponding to the D2-D3 expansion segment obtained from this study (PQ452334) and corresponding sequences from representative species in the *X. americanum*-group obtained from GenBank. In the phylogram (Figure 4), the *X. americanum* sequences demonstrated a dual clade pattern, which has also been reported in previous taxonomic studies of nematodes in this group (Archidona-Yuste et al. 2016; Gutiérrez-Gutiérrez et al. 2012; Troccoli et al. 2024). *X. rivesi* sequence from our study aligned with *X. rivesi* sequences in clade I. Based on the morphometric data and phylogenetic analysis of D2-D3 expansion segment, it can be concluded that *X. rivesi* is the dagger nematode species present in the blueberry field.

Nematode-mediated transmission of TRSV

X. rivesi adults collected from soil samples were tested by RT-PCR for the presence of TRSV. An approximately 372 bp fragment corresponding to the Hel region was amplified from a pooled sample of four nematodes but not in single nematode samples. We were unable to amplify sequences specific to RNA2 from either single or pooled nematode samples. This could be due to the presence of low quantities of TRSV genome segments in individual nematodes undetectable by PCR at the time of sampling. The amplicons generated from pooled nematode samples were sequenced by Sanger

sequencing. The derived sequences (PV066170 to PV066176) showed up to 98% nt sequence identity with corresponding sequence of RNA1 of TRSV isolate WA-AM1 (MW495243), indicating acquisition of the virus by *X. rivesi*.

To test whether *X. rivesi* could transmit TRSV from infected blueberry plants, a cucumber bait plant assay was conducted in 2019 and 2020 seasons. Cucumber (*C. sativus*, cv. Boston Pickling) seedlings were planted in two locations in the field where symptomatic, TRSV-positive blueberry plants were present. Distinct virus-like symptoms were observed in newly emerged leaves of the cucumber bait plants, starting around two months post-planting. These symptoms included chlorotic spots, ringspots, and leaf crinkling (Figure 5). After four months post-planting, all cucumber bait plants showed symptoms in both seasons and tested positive for TRSV in RT-PCR assays. Sanger sequencing of an approximately 372 bp amplicon specific to the Hel region (PV237153 to PV237157) from five TRSV-positive cucumber plants showed a maximum of 99% nt sequence identity with corresponding sequence of RNA1 of TRSV isolate WA-AM1 (MW495243). Sanger sequencing of an approximately 650 bp amplicon specific to a portion of the CP (PV237143 to PV237152) from ten TRSV-positive cucumber plants () showed a maximum of 91% nt sequence identity with corresponding sequence of RNA2 of isolate WA-MR1 (MW495244). To further confirm these results, the total RNA isolated from five symptomatic cucumbers collected in 2020 were subjected to Illumina sequencing. As shown in Table 3, an average of 2,019,121 and 1,610,146 reads were mapped, respectively, to TRSV RNA1 and RNA2 segments. *De novo* assembly of these TRSV-specific reads resulted in five contigs corresponding to RNA1 (sizes between 6,782 and 7,316 bp; average coverage = 41,476.4) and five contigs corresponding to RNA2

(sizes between 3,251 and 3606 bp; average coverage = 59,791.1). The contigs specific to RNA1 (PV237158 to PV237162) and RNA2 (PV237163 to PV237167) shared, respectively, a maximum of 96.4% and 91.1% nt sequence identity with RNA1 (MW495243) and RNA2 (MW495244) of TRSV isolate WA-AM1.

Discussion

In this study, the genome of a TRSV isolate infecting highbush blueberry was characterized at the molecular level using a combination of high-throughput sequencing and Sanger sequencing. The complete sequence of RNA1 and RNA2 genome segments of the TRSV isolate was determined to be 7,512 nt and 3,925 nt, respectively. Phylogenetic analysis confirmed TRSV as a distinct member of sub-group A unlike other blueberry-infecting nepoviruses that belong to sub-group C (Thompson et al. 2017). In the USA, TRSV has previously been reported in highbush blueberries in Arkansas, Connecticut, Illinois, Michigan, New York, Oregon, and New Brunswick (Converse and Ramsdell 1982; Fuchs et al. 2010; Martin et al. 2012). In the Pacific Northwest, only tomato ringspot virus (ToRSV), in addition to the more common BISHV and BISCv, was reported to date in blueberry plantings (Martin and Tzanetakis 2018). This study, together with a previous report (Mitra et al. 2021), has established TRSV as a potential threat to blueberry production in Washington state.

Based on the negative impacts of TRSV in blueberries reported in this study, it is evident that the virus has an adverse impact on blueberry production. Likewise, adverse effects of the virus on production of other fruit crops, legumes and horticultural crops have

been documented (Stace-Smith and Hansen 1974, Uyemoto et al. 1977, Stone 1980, Tolin 2008, Martin et al. 2013, Fuchs et al. 2021). It is also interesting to note that TRSV can cause asymptomatic infections in melon fruits with little to no impact on fruit yield and quality (Tabara et al. 2021). Additional studies on genetic variability in blueberry-infecting TRSV populations relative to non-blueberry-infecting populations across different hosts and geographical regions will further expand our knowledge on epidemiologically important evolutionary processes of the virus.

Although reasons behind the occurrence of TRSV in the blueberry field are not yet clear, anecdotal information from the grower indicated that the current field was barren until planting with blueberries, which raises the possibility that the virus might have been introduced through infected planting stock. Since the grower purchased blueberry plants from a nursery (name withheld due to confidentiality) for planting in 2015, it can be argued that TRSV was introduced through infected plants leading to virus establishment in the newly planted field. Once established, the nematodes could transmit TRSV from infected plants to healthy neighbors during their feeding on roots. Since TRSV and *X. rivesi* both have broad host ranges, including perennial crops and several weed species (EPPO 2024), an alternative hypothesis would be that both the virus and the nematode vector persisted on susceptible weed species present in the field during the fallow period and the blueberry plants became infected with TRSV during nematode vector feeding after planting.

From a practical point of view, our results highlight the critical need for examining soils for freedom from nematode vectors before planting and sourcing blueberry plants tested free from TRSV and other harmful viruses for new plantings. Since TRSV naturally

infects a wide range of herbaceous and woody hosts (Wintermantel 2017) and *X. rivesi* is widely present in Washington soils (Akinbade et al. 2014; Olaya et al. 2024), the virus can cause serious diseases in several crops when introduced, including grapevines, small fruit and , tree fruit crops (Schilder et al. 2003; Šubíková et al. 2002; Martin et al. 2012; Walker et al. 2015). In view of the widespread occurrence of dagger nematode vectors in small fruits and wine grapes in the Pacific Northwest (Olaya et al., 2024), more studies are needed to determine whether the presence of TRSV currently reported (Mitra et al. 2021; Walker et al. 2015; this study) represents isolated cases or if the virus is widely distributed yet undetected in small fruits within the state and across the Pacific Northwest region.

Besides dagger nematode vectors and clonal propagation of infected plants, TRSV spread via seed and pollen (Wintermantel 2017) has implications in the epidemiology of the virus. Since insect pollinators, such as honeybees, are widely used by growers for blueberry pollination and a recent study reported pollen carried by honeybees contained nepoviruses (Lee et al. 2023), the potential role of insect pollinators while foraging during bloom in pollen-mediated spread of TRSV from infected plants to neighboring healthy plants in bee-pollinated blueberry fields warrants further investigation.

Cucumbers have been used previously as a bait plant host for demonstrating the transmission of nematode-borne viruses (Širca et al. 2007). In this study, the cucumber baiting technique was used by growing healthy cucumber seedlings near symptomatic blueberry plants and testing bait plants by RT-PCR to demonstrate that TRSV is transmissible by soil-borne dagger nematodes. Identification of adult female nematodes collected from the soil using morphometric and molecular taxonomy methods and the

detection of TRSV in nematodes confirmed *X. rivesi* as a vector of the virus. Additional studies on the transmission of TRSV via *X. rivesi* to both cultivated and wild blueberry species may allow further research on cultivar-specific responses to the virus and identification of resistance genes to the nematode vector and the virus. At present, roguing infected plants and plant certification programs are the primary strategies for mitigating virus diseases in several perennial fruit crops. Soil-borne nematodes that act as virus vectors, however, pose an additional challenge to management of economically important virus diseases. Soil fumigation is a major control strategy against virus-vectoring nematodes. However, in organic farming of blueberries, fumigation is not a practical option. In this scenario, cultural control measures could be implemented to manage dagger nematode vectors. Some cultural control strategies include using shoe covers when working in nematode-infested fields, sanitizing tools and restricting field movement of vehicles from infested fields to non-infested areas, removing weeds that support the virus or vector, roguing of infected bushes, and sourcing virus-tested plants from certified nurseries (Westphal 2011).

Acknowledgements

This project was funded by the Washington State University Agricultural Research Center and the USDA National Institute for Food and Agriculture Hatch Project Number: WNP00006.

Literature Cited

- Adiputra, J., Kesoju, S. R., and Naidu, R. A. 2018. The Relative Occurrence of *Grapevine leafroll-associated virus 3* and *Grapevine red blotch virus* in Washington State Vineyards. *Plant Disease*. 102 (11), 2129-2135.
- Akinbade, S. A., Mojtahedi, H., Guerra, L., Eastwell, K., Villamor, D. E. V., Handoo, Z. A., and Skantar, A. M. 2014. First Report of *Xiphinema rivesi* (Nematoda, Longidoridae) in Washington State. *Plant Disease*. 98 (7), 1018-1018.
- Alabi, O. J., Kumar, P. L., and Naidu, R. A. 2008. Multiplex PCR for the detection of *African cassava mosaic virus* and *East African cassava mosaic Cameroon virus* in cassava. *Journal of Virological Methods*. 154 (1-2), 111-120.
- Alabi, O. J., Casassa, L. F., Gutha, L. R., Larsen, R. C., Henick-Kling, T., Harbertson, J.F., and Naidu, R. A. 2016. Impacts of Grapevine Leafroll Disease on Fruit Yield and Grape and Wine Chemistry in a Wine Grape (*Vitis vinifera* L.) Cultivar. *PLoS One*. 11 (2), e0149666.
- Archidona-Yuste, A., Navas-Cortés, J. A., Cantalapiedra-Navarrete, C., Palomares-Rius, J. E., and Castillo, P. 2016. Cryptic diversity and species delimitation in the *Xiphinema americanum*-group complex (Nematoda: Longidoridae) as inferred from morphometrics and molecular markers. *Zoological Journal of the Linnean Society*, 176 (2), 231-265.
- Buckley, B., Silva, S., and Singh, S. 1993. Nucleotide sequence and in vitro expression of the capsid protein gene of tobacco ringspot virus. *Virus Research*. 30 (3), 335-349.
- Buzayan, J. M., Gerlach, W. L., and Bruening, G. 1986. Satellite tobacco ringspot virus RNA: A subset of the RNA sequence is sufficient for autolytic processing. *Proceedings of the National Academy of Sciences*. 83 (23), 8859-8862.
- Carrier, K. J. 1999. Cleavage site specificity of the tomato ringspot nepovirus protease (Doctoral dissertation, University of British Columbia).
- Carta, L. K., Handoo, Z. A., Li, S., Kantor, M., Bauchan, G., McCann, D., Gabriel, C. K., Yu, Q., Reed, S., Koch, J., and Martin, D. 2020. Beech leaf disease symptoms caused by newly recognized nematode subspecies *Litylenchus crenatae mccannii* (Anguinata) described from *Fagus grandifolia* in North America. *Forest Pathology*. 50 (2), e12580.
- Chandrasekar, V. and Johnson, J. E. 1998. The structure of tobacco ringspot virus: a link in the evolution of icosahedral capsids in the picornavirus superfamily. *Structure*. 6 (2), 157-171.
- Converse, R. H. and Ramsdell, D. C. 1982. Occurrence of Tomato and Tobacco Ringspot Viruses and of Dagger and Other Nematodes Associated with Cultivated Highbush Blueberries in Oregon. *Plant Disease*. 66 (8), 710-712.

- Courtney, R. and Mullinax, T. J. 2020. Big time for blueberries. Good Fruit Grower. Retrieved from <https://www.goodfruit.com/big-time-for-blueberries/>. (Last accessed April 19, 2024)
- Dalmasso, A. 1969. Anatomical studies and taxonomy of the genera *Xiphinema*, *Longidorus* and *Paralongidorus* (Nematoda: Dorylaimidae). Memoires du Museum Nationale d'Histoire Naturelle, Série A, Zoologie. 61 (2), 33-82.
- de Man, J. G. 1877. Onderzoekingen over vrij in de aarde levende Nematoden (Vol. 1).
- Demangeat, G., Komar, V., Cornuet, P., Esmenjaud, D., and Fuchs, M. 2004. Sensitive and reliable detection of grapevine fanleaf virus in a single *Xiphinema index* nematode vector. Journal of Virological Methods. 122 (1), 79-86.
- DeVetter, L. W., Granatstein, D., Kirby, E., and Brady, M. 2015. Opportunities and Challenges of Organic Highbush Blueberry Production in Washington State. HortTechnology. 25 (6), 796-804.
- Digiario, M., Elbeaino, T., and Martelli, G. P. 2007. Development of degenerate and species-specific primers for the differential and simultaneous RT-PCR detection of grapevine-infecting nepoviruses of subgroups A, B and C. Journal of Virological Methods. 141 (1), 34-40.
- Edgar, R. C. 2004. MUSCLE: multiple sequence alignment with high accuracy and high throughput. Nucleic Acids Research. 32 (5), 1792-1797.
- EPPO 2024. *Xiphinema rivesi*. EPPO datasheets on pests recommended for regulation. <https://gd.eppo.int>. (Last accessed September 21, 2024)
- Fadaei, A. A., Coomans, A., and Kheiri, A. 2003. Three species of the *Xiphinema americanum* lineage (Nematoda: Longidoridae) from Iran. Nematology, 5 (3), 453-461.
- Farahnaz, J. A., Fatemeh, S., Ali, M. B., Castillo, P., Mirzaie, F. Z., and Majid, P. 2020. Occurrence of *Xiphinema santos Lambertii*, Lemos, Agostinelli & D'Addabo 1993 (Nematoda: Longidoridae), a *X. americanum*-group member in Iran. European Journal of Plant Pathology. 157 (2), 281-291.
- Fouladvand, Z. M., Pourjam, E., Castillo, P., and Pedram, M. 2019. Genetic diversity, and description of a new dagger nematode, *Xiphinema afratakhtehnsis* sp. nov., (Dorylaimida: Longidoridae) in natural forests of southeastern Gorgan, northern Iran. PLoS One. 14 (5), e0214147.
- Fromme, F. D., Wingard, S. A., and Priode, C.N. 1927. Ringspot of Tobacco: an infectious disease of unknown cause. Phytopathology. 17 (5).
- Fuchs, M., Abawi, G. S., Marsella-Herrick, P., Cox, R., Cox, K. D., Carroll, J. E., and Martin, R. R. 2010. Occurrence of *Tomato ringspot virus* and *Tobacco ringspot virus* in highbush blueberry in New York State. Journal of Plant Pathology. 92 (2), 451-459.

- Fuchs, M., Schmitt-Keichinger, C., and Sanfaçon, H. 2017. A Renaissance in Nepovirus Research Provides New Insights into their Molecular Interface with Hosts and Vectors. *Advances in Virus Research*. 97, 61-105.
- Fuchs, M., Almeyda, C. V., Al Rwahnih, M., Atallah, S. S., Cieniewicz, E. J., Farrar, K., Foote, W. R., Golino, D. A., Gómez, M. I., Harper, S. J., and Kelly, M.K. 2021. Economic Studies Reinforce Efforts to Safeguard Specialty Crops in the United States. *Plant Disease*. 105 (1), 14-26.
- Gilmer, R. M., Uyemoto, J. K., and Kelts, L. J. 1970. A new grapevine disease induced by tobacco ringspot virus. *Phytopathology*. 60, 619-27.
- Golden, A. M. 1990. Preparation and mounting nematodes for microscopic observation. *Plant nematology laboratory manual*. Amherst, MA: University of Massachusetts Agricultural Experiment Station. 197-205.
- Gutha, L. R., Casassa, L. F., Harbertson, J. F., and Naidu, R. A. 2010. Modulation of flavonoid biosynthetic pathway genes and anthocyanins due to virus infection in grapevine (*Vitis vinifera* L.) leaves. *BMC Plant Biology*, 10, 1-18.
- Gutiérrez-Gutiérrez, C., Cantalapiedra-Navarrete, C., Decraemer, W., Vovlas, N., Prior, T., Rius, J. E. P., & Castillo, P. 2012. Phylogeny, diversity, and species delimitation in some species of the *Xiphinema americanum*-group complex (Nematoda: Longidoridae), as inferred from nuclear and mitochondrial DNA sequences and morphology. *European Journal of Plant Pathology*, 134, 561-597.
- Handoo, Z. A., Ibrahim, I. K. A., Chitwood, D. J., and Mokbel, A. A. 2015. First report of *Xiphinema rivesi* Dalmasso, 1969 on citrus in northern Egypt. *Pakistan Journal of Nematology*. 33 (2), 161-165.
- Hooper, D. J. 1970. Handling, fixing, staining and mounting nematodes. *Laboratory Methods for Work with Plant and Soil Nematodes*. 5th ed., J. F. Southey, ed. Her Majesty's Stationery Office, London, 39-54.
- Illand, P., Ewart, A., Sitters, J., Markides, A., and Bruer, N. 2000. Techniques for chemical analysis and quality monitoring during wine making. *Patrick Illand Wine Promotions*, Campbelltown, 111.
- Jairajpuri, M. S. and Ahmad, W. 1992. *Dorylaimida: Free-living, Predaceous and Plant-parasitic Nematodes*. New Delhi, India: Oxford & IBH Publishing Co.
- Jenkins, W. 1964. A rapid centrifugal-flotation technique for separating nematodes from soil. *Plant Disease Reporter*. 48 (9), 692.
- Kantor, M. R., Handoo, Z. A., Skantar, A. M., Hult, M. N., Ingham, R. E., Wade, N. M., Ye, W., Bauchan, G. R., and Mowery, J. D. 2020. Morphological and molecular characterisation of *Punctodera mulveyi* n. sp. (Nematoda: Punctoderidae) from a golf

- course green in Oregon, USA, with a key to species of *Punctodera*. *Nematology*. 23 (6), 667-683.
- King, A. M. Q., Adams, M. J., Carstens, E. B., and Lefkowitz, E.J. 2012. Ninth Report of the International Committee on Taxonomy of Viruses. San Diego, California USA: Elsevier.
- Kumar, S., Stecher, G., Li, M., Knyaz, C., and Tamura, K. 2018. MEGA X: Molecular Evolutionary Genetics Analysis across Computing Platforms. *Molecular Biology and Evolution*. 35 (6), 1547-1549.
- Lamberti, F. and Carone, M. 1991. A dichotomous key for the identification of species of *Xiphinema* (Nematoda: Dorylaimida) within the *X. americanum*-group. *Nematologia Mediterranea*. 19 (2), 341-348.
- Le, S. Q. and Gascuel, O. 2008. An Improved General Amino Acid Replacement Matrix. *Molecular Biology and Evolution*. 25 (7), 1307-1320.
- Lee, E., Vansia, R., Phelan, J., Lofano, A., Smith, A., Wang, A., Bilodeau, G.J., Pernal, S.F., Guarna, M.M., Rott, M., and Griffiths, J. S. 2023. Area Wide Monitoring of Plant and Honey Bee (*Apis mellifera*) Viruses in Blueberry (*Vaccinium corymbosum*) Agroecosystems Facilitated by Honey Bee Pollination. *Viruses*. 15 (5), 1209.
- Lefkowitz, E. J., Dempsey, D. M., Hendrickson, R. C., Orton, R. J., Siddell, S. G., and Smith, D. B. 2018. Virus taxonomy: the database of the International Committee on Taxonomy of Viruses (ICTV). *Nucleic Acids Research*. 46 (D1), D708-D717.
- Loof, P. A. A. and Luc, M. 1993. A revised polytomous key for the identification of species of the genus *Xiphinema* Cobb, 1913 (Nematoda: Longidoridae) with exclusion of the *X. americanum*-group: Supplement 1. *Systematic Parasitology*. 24 (3), 185-189.
- Maclot, F. J., Debue, V., Blouin, A. G., Pareta, N. F., Tamisier, L., Filloux, D., and Massart, S. 2021. Identification, molecular and biological characterization of two novel secovirids in wild grass species in Belgium. *Virus Research*. 298, 198397.
- Mai, W. F. and Lyon, H. H. 1975. Pictorial Key to the Genera of Plant-Parasitic Nematodes. 4th ed. Ithaca, NY, USA: Cornell University Press.
- Martin, R. R., Polashock, J. J., and Tzanetakis, I. E. 2012. New and Emerging Viruses of Blueberry and Cranberry. *Viruses*. 4 (11), 2831-2852.
- Martin, R. R., MacFarlane, S., Sabanadzovic, S., Quito, D., Poudel, B., and Tzanetakis, I. E. 2013. Viruses and Virus Diseases of *Rubus*. *Plant Disease*, 97 (2), 168-182.
- Martin, R. R. and Tzanetakis, I. E. 2018. High Risk Blueberry Viruses by Region in North America; Implications for Certification, Nurseries, and Fruit Production. *Viruses*. 10 (7), 342.

- McGuire, J. M., Kim, K. S., and Douthit, L. B. 1970. Tobacco ringspot virus in the nematode *Xiphinema americanum*. *Virology*. 42 (1), 212-216.
- Menzel, W., Jelkmann, W., and Maiss, E. 2002. Detection of four apple viruses by multiplex RT-PCR assays with coamplification of plant mRNA as internal control. *Journal of Virological Methods*. 99 (1-2), 81-92.
- Mink, G. I. 1993. Pollen and seed-transmitted viruses and viroids. *Annual Review of Phytopathology*. 31 (1), 375-402.
- Mitra, A., Jarugula, S., Hoheisel, G., and Naidu, R. A. 2021. First Report of Tobacco Ringspot Virus in Highbush Blueberry in Washington State. *Plant Disease*. 105 (9), 2739.
- NASS, 2022. Press Release. [FRUIT.pdf](https://www.nass.usda.gov/Statistics_by_State/Idaho/Publications/Census_Press_Releases/2023/FRUIT.pdf).
https://www.nass.usda.gov/Statistics_by_State/Idaho/Publications/Census_Press_Releases/2023/FRUIT.pdf (accessed on January 6, 2025).
- Nei, M. and Kumar, S. 2000. *Molecular evolution and phylogenetics*. Oxford university press.
- Owusu, G. K., Crowley, N. C., and Francki, R. I. B. 1968. Studies of the seed-transmission of Tobacco ringspot virus. *Annals of Applied Biology*. 61 (2), 195-202.
- Olaya, C., Reinhold, L., Platt, M., Peetz, A., Donahue, K., and Zasada, I. 2024. Assessment of the Distribution of Dagger Nematodes and Associated Nematode Transmitted Viruses in Pacific Northwest Small Fruit Crops. *Plant Health Progress*. 25 (4).
- Price, W. C. 1940. Comparative Host Ranges of Six Plant Viruses. *American Journal of Botany*. 27 (7), 530-541.
- Rezaian, M. A. and Jackson, A. O. 1981. Low-Molecular-Weight RNAs Associated with Tobacco Ringspot Virus Are Satellites. *Virology*. 114 (2), 534-541.
- Rowhani, A., Daubert, S. D., Uyemoto, J. K., Al Rwahnih, M., and Fuchs, M. 2017. American Nepoviruses. *Grapevine Viruses: Molecular Biology, Diagnostics and Management*. Springer, Cham, 109-126.
- Sanfaçon, H., Wellink, J., Le Gall, O., Karasev, A., van der Vlugt, R., and Wetzel, T. 2009. Secoviridae: a proposed family of plant viruses within the order *Picornavirales* that combines the families *Sequiviridae* and *Comoviridae*, the unassigned genera *Cheravirus* and *Sadwavirus*, and the proposed genus *Torradovirus*. *Archives of Virology*. 154, 899-907.
- Schilder, A. M. C., Gillett, J. M., Byrne, J. M., and Zabadal, T. J. 2003. First Report of *Tobacco ringspot virus* in Table Grapes in Michigan. *Plant Disease*. 87 (9), 1149.

- Schneider, I. R. 1971. Characteristics of a satellite-like virus of tobacco ringspot virus. *Virology*. 45 (1), 108-122.
- Schneider, I. R. and White, R. M. 1976. Tobacco ringspot virus codes for the coat protein of its satellite. *Virology*. 70 (1), 244-246.
- Širca, S., Stare, B. G., Pleško, I. M., Marn, M. V., Urek, G., and Javornik, B. 2007. *Xiphinema rivesi* from Slovenia Transmit *Tobacco ringspot virus* and *Tomato ringspot virus* to Cucumber Bait Plants. *Plant Disease*. 91 (6), 770-770.
- Skantar, A. M., Handoo, Z. A., Zanakis, G. N., and Tzortzakakis, E. A. 2012. Molecular and Morphological Characterization of the Corn Cyst Nematode, *Heterodera zae*, from Greece. *Journal of Nematology*. 44 (1), 58-66.
- Šneideris, D., Zitikaitė, I., Žižytė, M., Grigaliūnaitė, B., and Staniulis, J. 2012. Identification of nepoviruses in tomato (*Lycopersicon esculentum* Mill.). *Žemdirbystė= Agriculture*. 99 (2), 173-178.
- Stace-Smith, R. and Hansen, A. J. 1974. Occurrence of tobacco ringspot virus in sweet cherry. *Canadian Journal of Botany*. 52 (7), 1647-1651.
- Stace-Smith, R. 1985. Tobacco ringspot virus. AAB Descriptions of Plant Viruses. No. 309.
- Stone, O. M. 1980. Nine viruses isolated from pelargonium in the United Kingdom. V International Symposium on Virus diseases of Ornamental Plants. 110, 177-182.
- Šubíková, V., Kollerova, E. and Slovákova, Ľ. 2002. Occurrence of Nepoviruses in Small Fruits and Fruit Trees in Slovakia. *Plant Protection Science*. 38 (Special 2), 367-369.
- Tabara, M., Nagashima, Y., He, K., Qian, X., Crosby, K. M., Jifon, J., Jayaprakasha, G. K., Patil, B., Koiwa, H., Takahashi, H., and Fukuhara, T. 2021. Frequent asymptomatic infection with tobacco ringspot virus on melon fruit. *Virus Research*. 293, 198266.
- Thomas, W. K., Vida, J. T., Frisse, L. M., Mundo, M., and Baldwin, J. G. 1997. DNA Sequences from Formalin-Fixed Nematodes: Integrating Molecular and Morphological Approaches to Taxonomy. *Journal of Nematology*. 29 (3), 250-254.
- Thompson, J. R., Dasgupta, I., Fuchs, M., Iwanami, T., Karasev, A. V., Petrzik, K., Sanfaçon, H., Tzanetakis, I., van Der Vlugt, R., Wetzel, T. and Yoshikawa, N. 2017. ICTV virus taxonomy profile: Secoviridae. *Journal of General Virology*, 98 (4), 529-531.
- Tolin, S. A. 2008. Tobacco viruses. Elsevier, 60-67.
- Troccoli, A., Vovlas, A., Fanelli, E., Papeschi, V., Toninelli, S., D'Addabbo, T., and De Luca, F. 2024. Integrative characterization and phylogenetic relationships of *Xiphinema rivesi* and *X. pachtaicum* (Nematoda, Longidoridae) associated to vineyards in North Italy. *European Journal of Plant Pathology*, 169 (1), 137-157.

- Urek, G., Sirca, S., and Karssen, G. (2005). Morphometrics of *Xiphinema rivesi* Dalmasso, 1969 (Nematoda: Dorylaimida) from Slovenia. *Russian Journal of Nematology*, 13 (1), 13.
- Uyemoto, J. K., Welsh, M. F., and Williams, E. 1977. Pathogenicity of tobacco ringspot virus in cherry. *Phytopathology*. 67 (4), 439-441.
- Walker, L., Bagewadi, B., Schultz, A., and Naidu, R. A. 2015. First Report of *Tobacco ringspot virus* Associated With Fanleaf Disease in a Washington State Vineyard. *Plant Disease*, 99 (9), 1286.
- Wang, S., Gergerich, R. C., Wickizer, S. L., and Kim, K. S. 2002. Localization of Transmissible and Nontransmissible Viruses in the Vector Nematode *Xiphinema americanum*. *Phytopathology*. 92 (6), 646-653.
- Westphal, A. 2011. Sustainable Approaches to the Management of Plant-parasitic Nematodes and Disease Complexes. *Journal of Nematology*. 43 (2), 122-125.
- Williams, B. D., Schrank, B., Huynh, C., Shownkeen, R., and Waterston, R. H. 1992. A Genetic Mapping System in *Caenorhabditis elegans* Based on Polymorphic Sequence-Tagged Sites. *Genetics*. 131 (3), 609-624.
- Wintermantel, W. M. 2017. Tobacco ringspot virus. In: Keinath, A.P., Wintermantel, W.M., Zitter, T.A., editors. *Compendium of Cucurbit Diseases and Pests*. 2nd edition. St. Paul, MN: APS Press. p. 151-152.
- Wojtowicz, M. R., Golden, A. M., Forer, L. B., and Stouffer, R. F. 1982. Morphological Comparisons Between *Xiphinema rivesi* Daimasso and *X. americanum* Cobb Populations from the Eastern United States. *Journal of Nematology*. 14 (4), p.511-516.
- Yang, A. F. and Hamilton, R. I. 1974. The mechanism of seed transmission of tobacco ringspot virus in soybean. *Virology*. 62 (1), 26-37.
- Yang, J., Fang, D., Shen, J., Chen, X., and Gao, F. 2020. Molecular characterization of tobacco ringspot virus from *Iris ensata*. *European Journal of Plant Pathology*, 158 (3), 805-809.
- Zasada, I. A., Peetz, A., Howe, D. K., Wilhelm, L. J., Cheam, D., Denver, D. R., and Smythe, A. B. 2014. Using Mitogenomic and Nuclear Ribosomal Sequence Data to Investigate the Phylogeny of the *Xiphinema americanum* Species Complex. *PLoS One*. 9 (2), 90035.
- Zhao, F., Hwang, U. S., Lim, S., Yoo, R. H., Igori, D., Lee, S. H., Lim, H. S., and Moon, J. S. 2015. Complete genome sequence and construction of infectious full-length cDNA clones of tobacco ringspot *Nepovirus*, a viral pathogen causing bud blight in soybean. *Virus Genes*. 51 (1), 163-166.

Legend for Figures:

Figure 1. Virus-like symptoms observed in highbush blueberry in cv. Draper. A: symptomatic plant (right) showing severe defoliation with a few flowers compared to a healthy plant (left); B: small, unripe berries collected from a symptomatic plant (right) compared to berries collected from a healthy plant (left); C: chlorotic spots; D: chlorotic spots and red-colored rings with chlorotic centers; E: leaf crinkling, mottling in addition to the red rings and chlorotic spots; F: healthy, non-symptomatic leaf.

Figure 2. TRSV detection by multiplex RT-PCR assay. RT-PCR amplicons were resolved by electrophoresis in 1.0% agarose gels. Amplicons specific to RNA1, RNA2 and *nad5* gene are shown with arrowheads on right with their size indicated in parentheses. Lanes 1-10: samples collected from cv. Draper, Lanes 11-15: samples collected from cv. Top Shelf. Lanes 4 to 6, 9 to 13 and lane 15 represent symptomatic plants and lanes 1 to 3, 7 and 8, and 13 and 14 represent samples from non-symptomatic plants. A 181 bp DNA band corresponding to the plant *nad5* gene as an internal control was amplified in all samples. M: 1 kb-plus DNA molecular marker (ThermoFisher Scientific, MA, USA). A sample from a healthy grapevine (cv. Grenache) served as the negative (-) control and a sample from a TRSV-infected grapevine (cv. Grenache) served as the positive (+) control (Walker et al. 2015).

Figure 3. Genome organization and phylogenetic analyses of TRSV isolate WA-AM1. A: Schematic representation (to-scale) of the genome organization of Tobacco ringspot virus isolate WA-AM1. The red circle at the 5'-end of both genome segments represents the viral genome-linked protein (VPg). Vertical dotted-line arrows indicate the predicted polyprotein dipeptide cleavage sites. Individual protein domains are indicated for both

RNA1 and RNA2. P1A: proteinase cofactor, P2A: RNA replication-associated protein, Hel: helicase, Pro: viral 3C-like protease, Pol: RNA-dependent RNA polymerase, MP: movement protein, CP: coat protein, and A(n): 3'-terminal poly(A) tail. B: Maximum-likelihood (ML) phylogenetic tree constructed using the conserved RNA1 Pro-Pol region (between the signature 'CG' and 'GDD' motifs) of representative isolates of the genus *Nepovirus*. TRSV isolate WA-AM1 indicated in bold font. C: ML phylogenetic tree constructed using the conserved RNA2 CP region of representative isolates of the genus *Nepovirus*. TRSV isolate WA-AM1 indicated in bold font. In both phylogenetic trees, a total of 16 sequences were used and no outgroup was included (unrooted). Bootstrap replication support of >70% indicated at corresponding branch nodes. Phylograms were built in MEGAX (Kumar et al. 2018). (AeRSV: Aeonium ringspot virus, ArMV: Arabis mosaic virus, BRSV: Beet ringspot virus, BRV: Blackcurrant reversion virus, CNSV: Cycas necrotic stunt virus, GBLV: Grapevine Bulgarian latent virus, GCMV: Grapevine chrome mosaic virus, GFLV: Grapevine fanleaf virus, PBRV: Potato black ringspot virus, PRMV: Peach rosette mosaic virus, RCNVA: Red clover nepovirus A, SLSV: Soybean latent spherical virus, TBRV: Tomato black ring virus, ToRSV: Tomato ringspot virus, and TRSV: Tobacco ringspot virus).

Figure 4. Maximum-likelihood phylogram depicting evolutionary relationships between *Xiphinema rivesi* Dalmasso, 1969 (this study; bold underlined font) and other members of the *Xiphinema americanum*-group complex (GenBank) based on D2-D3 expansion segments of 28S rRNA sequence. An *X. index* accession (HG969307) was included as an outgroup. The two major clades of *X. americanum* sequences have been indicated, aligning with previous descriptions of phylogenetic relationships in this group (Archidona-

Yuste et al. 2016; Gutiérrez-Gutiérrez et al. 2012). Bootstrap replication support of >70% (from 1,000 bootstraps) is indicated at corresponding branch nodes. The phylogram was constructed in MEGAX using the General Time Reversible model. A discrete Gamma distribution was used to model evolutionary rate differences among sites (+G, parameter = 0.9338). The rate variation model allowed for some sites to be evolutionarily invariable ([+I], 30.18% sites).

Figure 5. Cucumber bait plant bioassay to test for TRSV transmission by *Xiphinema rivesi*. Virus-like symptoms in newly emerging cucumber (*Cucumis sativus*, cv. Boston Pickling) leaves near the four-month post-planting time point. Symptoms included apical leaf chlorosis, leaf crinkling (A), and ringspot symptoms typical of TRSV infection (B-D).

Table 1. Primers used in the multiplex RT-PCR assay for the detection of Tobacco ringspot virus (TRSV).

Primer	Sequence (5' to 3')	Coordinates	Purpose
Hel_F	GACTACTGAGCAACATTGCAACTTCC	3630-3655 ^a	RNA1-Helicase
Hel_R	GTCCCCTAACAGCATTGACTACC	3979-4001 ^a	
CP_F	GCTGATTGGCAGTGTATTGTTAC	2346-2368 ^a	RNA2-CP
CP_R	GTGTTCGCATCTGGTTTCAAATTGG	2968-2992 ^a	
<i>nad5-s</i>	GATGCTTCTTGGGGCTTCTTGTT	968-987 and 1836-1838 ^b	NADH dehydrogenase subunit 5 (internal control)
<i>nad5-as</i>	CTCCAGTCACCAACATTGGCATAA	1973-1996 ^b	

^aDesigned based on TRSV isolate infecting grapevine in Washington State (Mitra et al., 2021).

^bfrom Menzel et al. 2002. Primers also targeted corresponding sequence in blueberry (PV173276) and cucumber (PV173277) in this study.

Table 2. Impact of Tobacco ringspot virus on blueberry fruit quality attributes.^a

Sample	Average weight of individual berries (g)	Total soluble solids (°Brix)	pH	Titrateable acidity (g Tartaric acid/100 juice)	of ml	Total anthocyanins (mg/g berry weight)
Healthy	54.94±3.19	15.56±0.49	3.57±0.05	7.62±0.49		1.445±0.08
Infected	10.62±1.99	7.28±0.26	3.21±0.07	31.02±0.47		0.236±0.06
p-value	*2.44x10 ⁻⁶	*3.87x10 ⁻⁷	*0.0025	*5.59x10 ⁻¹⁰		*3.03x10 ⁻⁶

^aData presented as average of five replicates (25 berries/replicate) ± standard error. A two-tailed t-test was conducted to infer statistical significance. Significant differences between fruit from healthy and infected plants is indicated by an asterisk with p-value for significance at 0.05.

Table 3. Summary of High-Throughput Sequencing data analyses from symptomatic Blueberry and Cucumber samples.

Host	Blueberry	Cucumber-1	Cucumber-2	Cucumber-3	Cucumber-4	Cucumber-5
Sampling year	2018	2019	2019	2020	2020	2020
Number of reads	27,939,948	22,053,622	22,867,442	26,823,232	30,203,558	29,676,698
Average read length (nt)	150	151	151	151	151	151
Total number of reads after trim	27,939,880	22,050,385	22,865,655	26,796,161	30,149,693	29,633,375
Reference-guided mapping summary						
Total number of reads mapped to TRSV virus	103,880	4,423,596	720,192	12,389,940	35,338	577,266
Reads mapped to TRSV RNA1 ^a	78,497	2297947	417347	7082709	19353	278248
Reads mapped to TRSV RNA2 ^b	25,383	2125649	302845	5307231	15985	299018
TRSV RNA1 consensus sequence length (Percent coverage)	7,514 (99.7)	7,467 (99.3)	7,448 (99.1)	7,506 (99.8)	7,382 (98.2)	7,452 (99.1)
TRSV RNA2 consensus sequence length (Percent coverage)	3,929 (98.1)	3,826 (97.3)	3,800 (96.7)	3,865 (98.3)	3,842 (97.7)	3,861 (98.2)

^aTRSV RNA1 reference accession: NC_005097.1.

^bTRSV RNA2 reference accession: NC_005096.1.

Table 4. Morphometrics of adult female *Xiphinema rivesi* from the current study, compared with corresponding *X. rivesi* morphometrics reported in prior publications.

Characteristic/ratio ^a	Publication, geographic origin, host, and data format										
	Current Study	Fadaei et al. 2003	Handoo et al. 2015	Troccoli et al. 2024	Wojtowicz et al. 1982	Wojtowicz et al. 1982	Wojtowicz et al. 1982	Urek et al. 2005	Urek et al. 2005	Urek et al. 2005	Urek et al. 2005
	WA, USA	Iran	Egypt	Italy	PA, USA	PA, USA	VT, USA	Slovenia	Slovenia	Slovenia	Slovenia
	Blueberry	Citrus	Citrus	Grapevine	Peach	Apple	<i>Rubus</i> sp.	Peach	Persimmon	Cherry	Grapevine
	Mean ± SE (Range)	Mean ± SD (Range)	Mean ± SD (Range)	Mean ± SD (Range)	Value (Range)	Value (Range)	Value (Range)	Mean (Range)	Mean (Range)	Mean (Range)	Mean (Range)
N	20	13	10	18	-	-	-	25	25	25	11
L	2118.4 ± 55.0 (1745-2653)	1700 ± 0.08 (1500-1800)	1600.6 ± 75.5 (1480-1660)	1892.8 ± 133.4 (1607-2166.7)	1800 (1700-2000)	1800 (1700-1900)	2100 (1900-2200)	1860 (1510-2180)	1980 (1680-2320)	1920 (1630-2140)	1960 (1780-2070)
a	55.9 ± 2.5 (41.55-73.69)	44.7 ± 2.9 (38.5-50)	35.1 ± 1.3 (32.7-37)	49.4 ± 2.1 (45.3-53.5)	50 (48-53)	47 (42-54)	40 (39-42)	47.97 (37.61-55.68)	48.39 (37.98-56.97)	51.07 (40.37-54.77)	45.39 (36.44-53.34)
b	8.5 ± 0.3 (6.68-11.43)	6.4 ± 0.5 (5.5-7)	6.6 ± 0.7 (5.5-7.4)	8.4 ± 0.7 (7.2-9.7)	6.4 (5.8-7.1)	6.7 (5.9-7.4)	7.1 (6.1-7.8)	5.93 (4.74-7.28)	6.30 (4.90-7.31)	6.33 (5.53-7.20)	6.00 (5.08-7.05)
c	62.9 ± 0.9 (55-70)	55.2 ± 3.0 (49.5-60)	56.0 ± 3.4 (50.2-59.5)	58.8 ± 5.5 (50.2-67.7)	56 (50-61)	56 (52-62)	64 (62-70)	55.24 (44.76-69.32)	55.73 (47.77-67.44)	55.62 (44.64-66.49)	57.95 (51.12-66.82)
c'	1.5 ± 0.1 (1.11-1.95)	1.3 ± 0.07 (1.2-1.4)	1.0 ± 0.1 (1.0-1.1)	1.4 ± 0.1 (1.2-1.7)	-	-	-	1.60 (1.40-1.76)	1.59 (1.36-1.83)	1.55 (1.33-1.78)	1.44 (1.27-1.59)
V%	52.2 ± 0.2 (50-54.2)	52.2 ± 0.7 (51-53.5)	52.1 ± 1.4 (50.4-54)	52.6 ± 0.9 (50.9-54.2)	52 (50-53)	53 (51-54)	52 (51-53)	53.5 (51.0-56.0)	53.4 (50.7-55.8)	53.2 (51.4-54.8)	53.5 (52.6-54.4)

Odontostyle length	83.4 ± 0.8 (80-90)	81.5 ± 2.8 (73.5-86)	87.5 ± 2 (85-90)	90.8 ± 2.3 (86.4-94.1)	90 (86-92)	92 (85-97)	94 (90-98)	90.9 (84.1-96.8)	92.8 (86.0-98.9)	90.1 (80.6-98.2)	91.9 (84.9-96.3)
Odontophore length	52.5 ± 0.5 (50-55)	46.2 ± 1.8 (42-48.5)	52.8 ± 2.9 (50-57)	51.2 ± 2.3 (48.4-56.1)	50 (48-51)	52 (49-55)	56 (51-62)	50.2 (42.0-53.5)	50.6 (40.9-54.5)	49.2 (43.9-53.2)	51.8 (48.1-55.4)
Total stylet length	135.8 ± 1.0 (130-145)	-	140.3 ± 3.8 (135-145)	-	140 (135-143)	145 (139-151)	149 (144-154)	141.1 (130.0-149.6)	143.4 (131.3-150.8)	138.9 (126.3-145.2)	143.7 (135.3-151.7)
Lip region diameter	10.7 ± 0.1 (10-12)	11.1 ± 0.4 (10.5-12)	-	8.9 ± 0.5 (8-9.9)	-	-	-	-	-	-	-
Lip region height	4.5 ± 0.1 (4-5)	-	-	-	-	-	-	-	-	-	-
Tail length	33.7 ± 0.8 (28-40)	30.8 ± 1.9 (28-33.5)	28.6 ± 1.9 (25-30)	32.4 ± 2.8 (28.4-38.9)	33 (31-34)	32 (30-34)	32 (30-34)	33.8 (29.0-39.6)	35.7 (32.0-43.1)	34.7 (29.2-40.3)	34.0 (30.4-37.9)
J (Hyaline portion of tail)	8.8 ± 0.5 (5-13)	9.4 ± 0.8 (8-11)	9.1 ± 1.5 (8-12)	8.3 ± 1.2 (5.8-11.6)	7.6 (6.9-8.2)	6 (4.3-8.2)	7.2 (5.6-8.6)	-	-	-	-
J diameter	10.3 ± 0.3 (8-13)	10.9 ± 0.8 (10-12.5)	12.6 ± 1.2 (11.5-15)	10.4 ± 1.0 (8.8-11.8)	10 (9-11)	11 (7.7-14)	14 (13-16)	-	-	-	-
Body width	38.8 ± 1.1 (30-48)	38.2 ± 3.3 (33.5-46.5)	45.7 ± 3.3 (40-50)	38.3 ± 3.1 (33.8-43.5)	-	-	-	39.0 (32.1-46.8)	41.4 (32.8-50.6)	37.9 (30.3-48.1)	43.8 (34.4-52.7)
Body diameter at anus	23.1 ± 0.4 (20-27)	23.2 ± 1.1 (21.5-25)	27.7 ± 1.6 (25-30)	23.8 ± 1.9 (21.1-28.4)	24 (22-25)	24 (19-28)	30 (28-31)	-	-	-	-
Body diameter at base of pharynx	32.1 ± 0.7 (27.5-38)	-	-	-	-	-	-	-	-	-	-
Anterior end to guide ring	68.2 ± 1.0 (55-77.5)	66.2 ± 2.0 (63-70)	72.2 ± 4 (65-75)	76.8 ± 2.6 (72.2-84.5)	68 (65-71)	75 (74-78)	79 (62-88)	80.0 (69.5-86.6)	80.8 (74.5-87.4)	78.9 (50.9-87.4)	78.6 (74.4-84.2)

Anterior end to vulva	1105.1 ± 27.4 (900-1361)	-	-	-	-	-	-	-	-	-	-
Anterior end to end of pharynx	254.4 ± 8.8 (210-325)	-	-	-	-	-	-	-	-	-	-

^aAll measurements are in μm . a: total body length/maximum body diameter, b: total body length/length from anterior end to end of pharynx, c: total body length/tail length, c': tail length/body diameter at anus, V%: (length from anterior end to vulva/total body length) x100 (Fouladvand et al. 2019; Jairajpuri and Ahmad 1992).

Figure 1

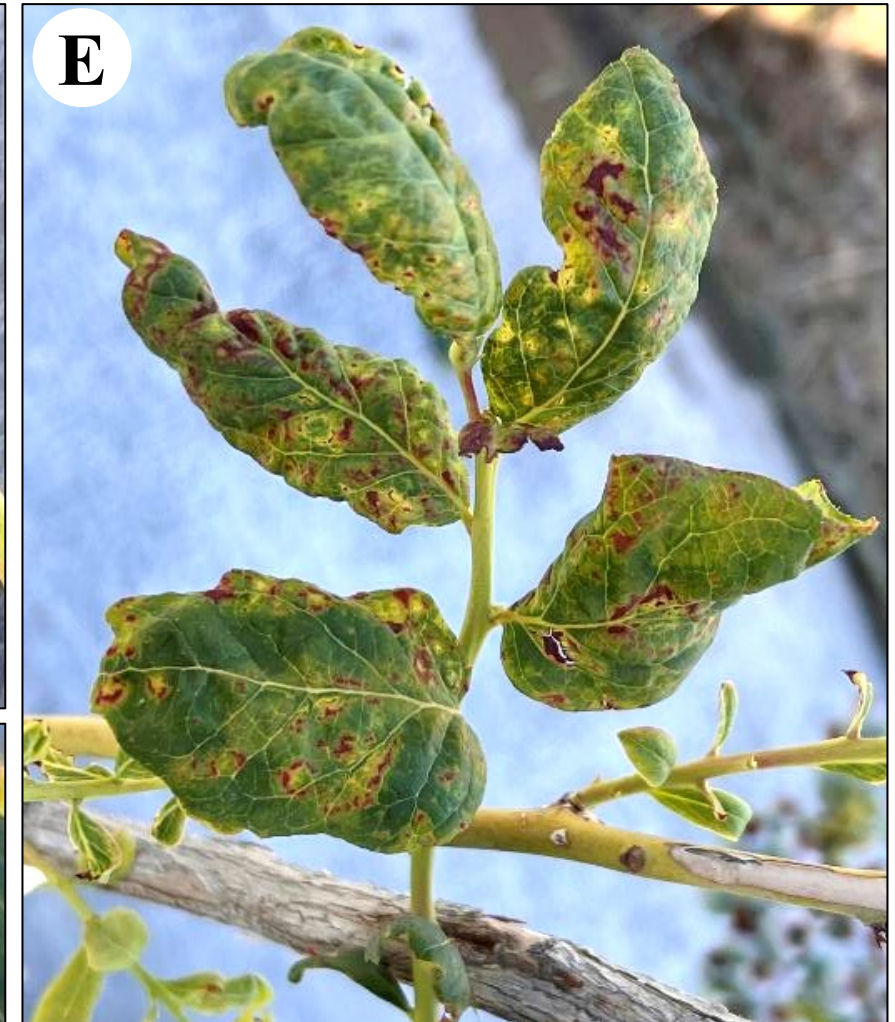


Figure 2

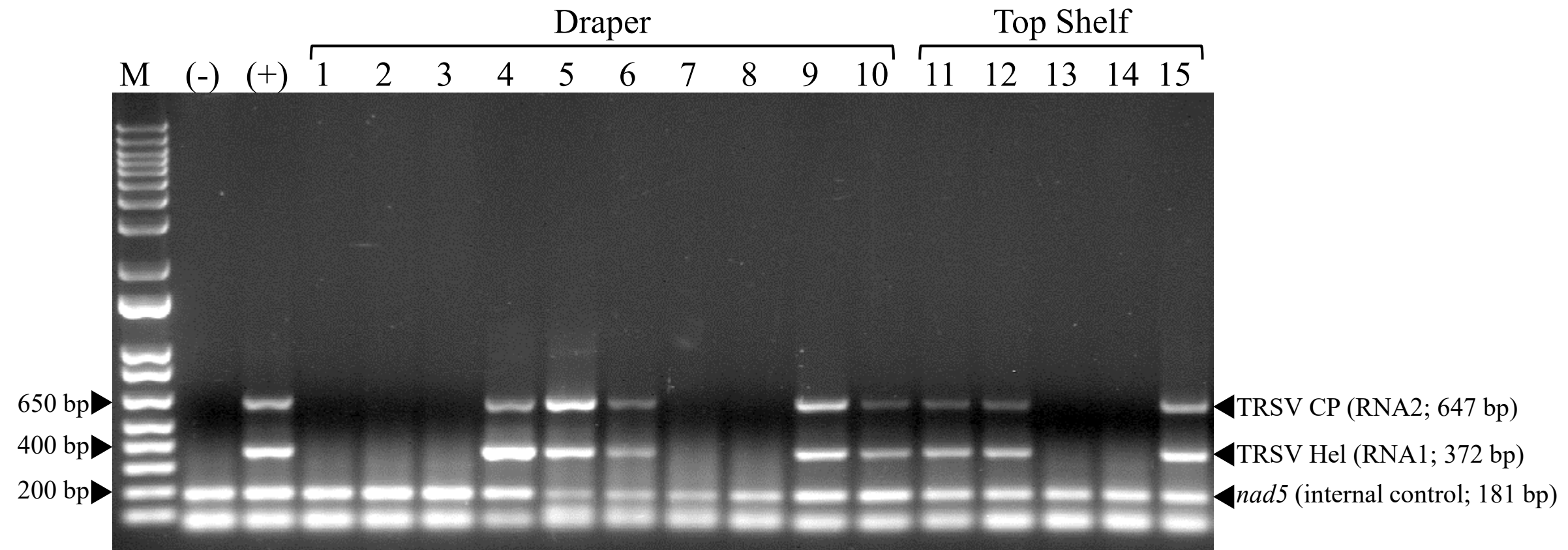


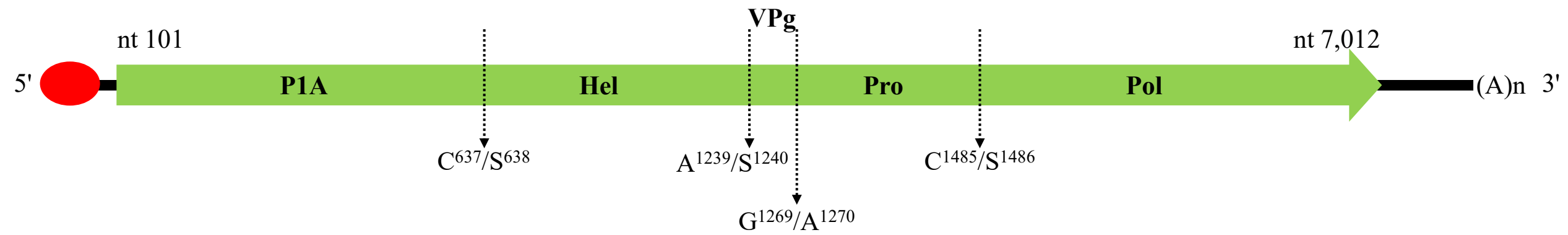
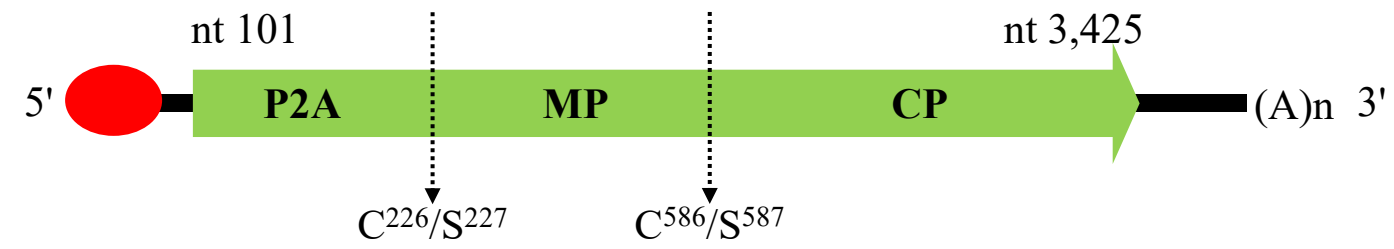
Figure 3A**RNA1 – 7,512 nt****RNA2 – 3,925 nt**

Figure 3B

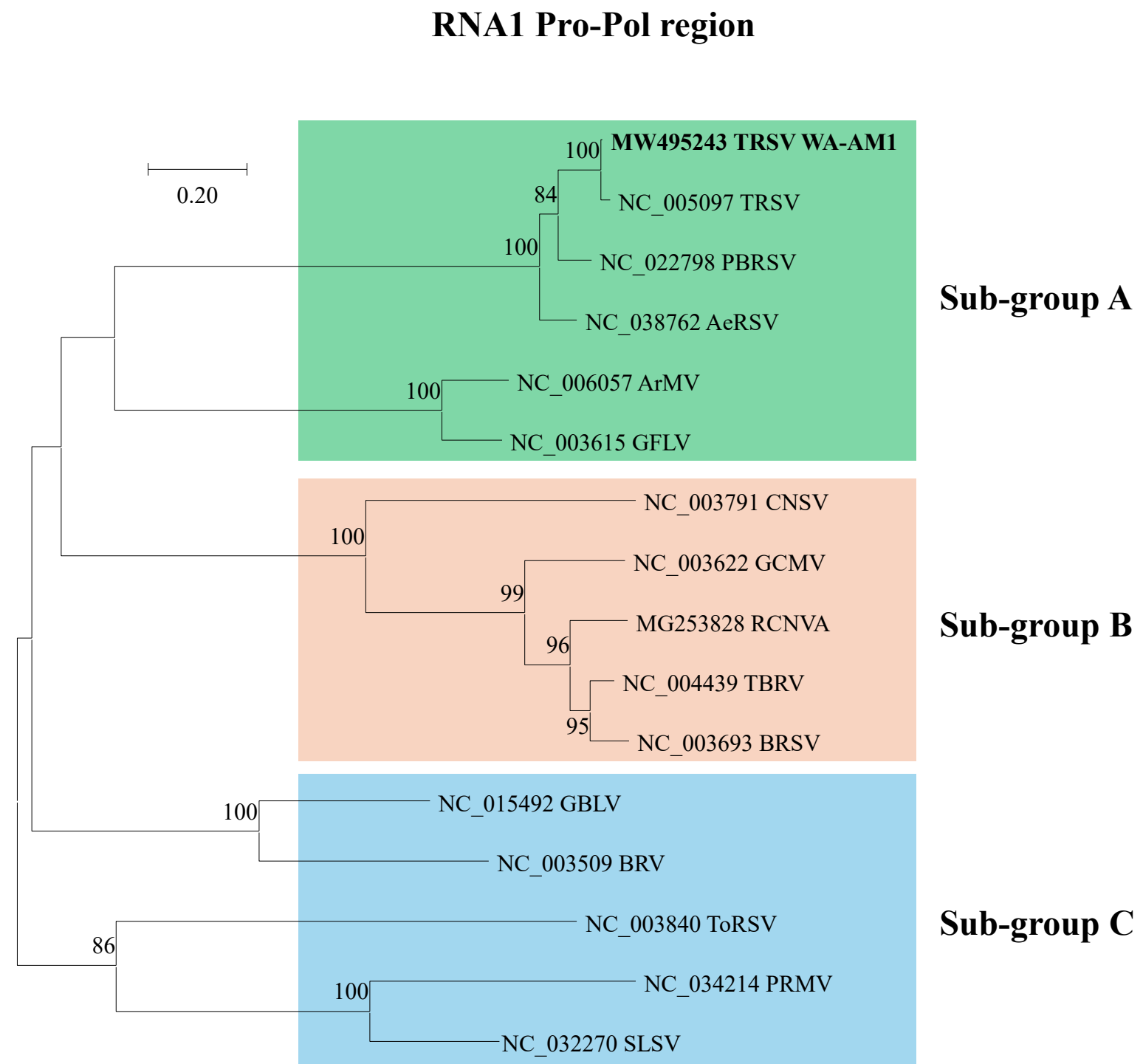
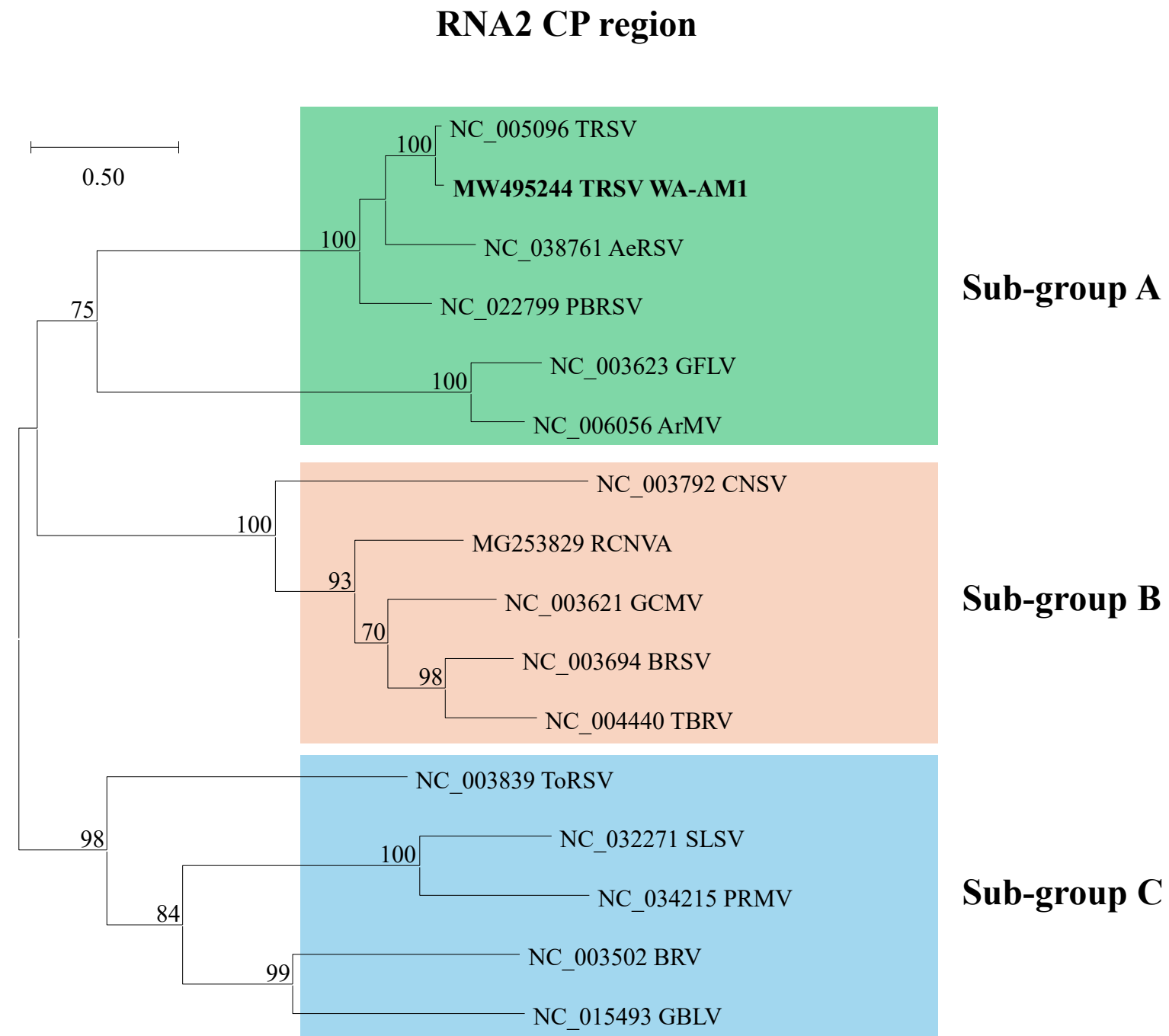
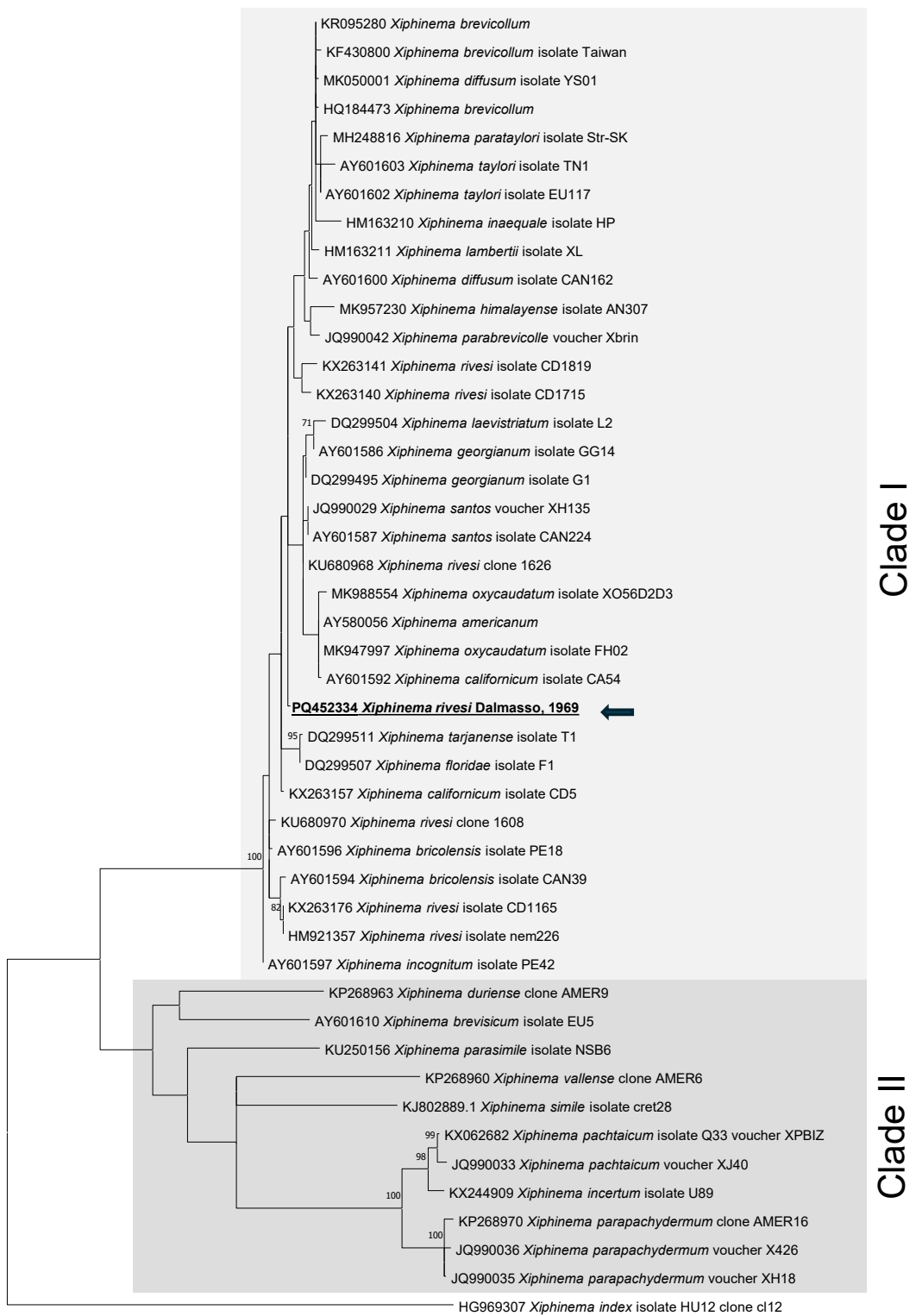


Figure 3C

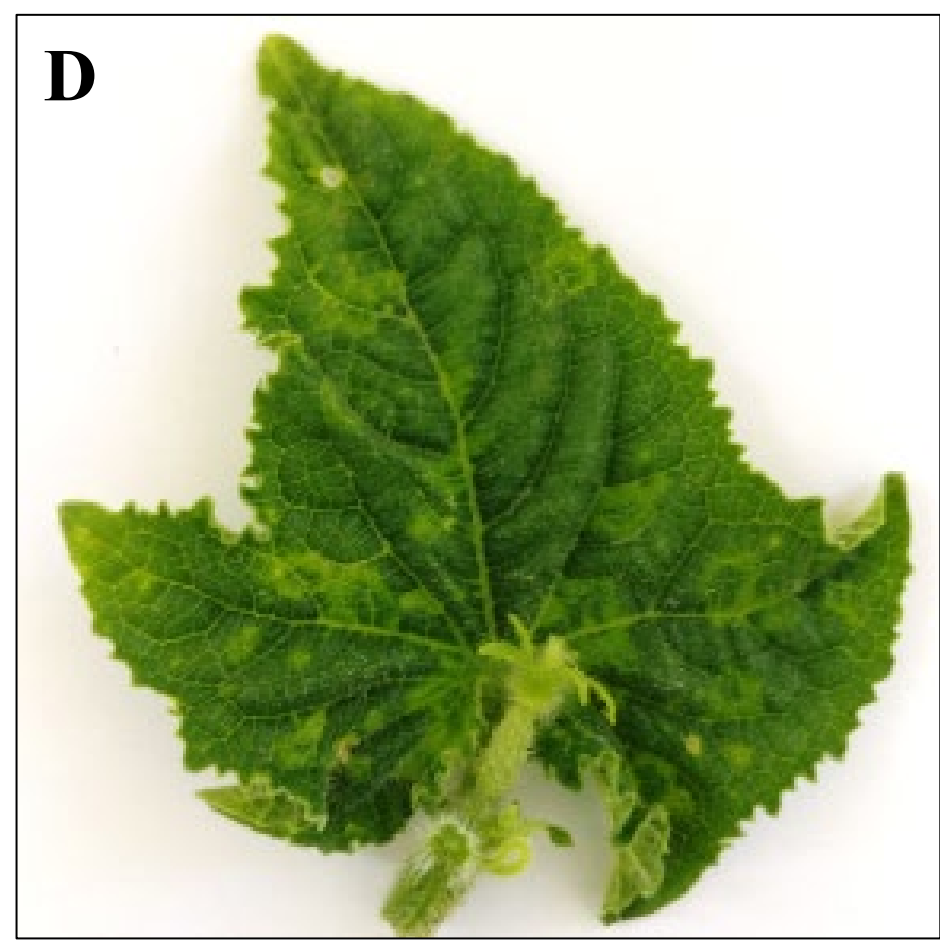
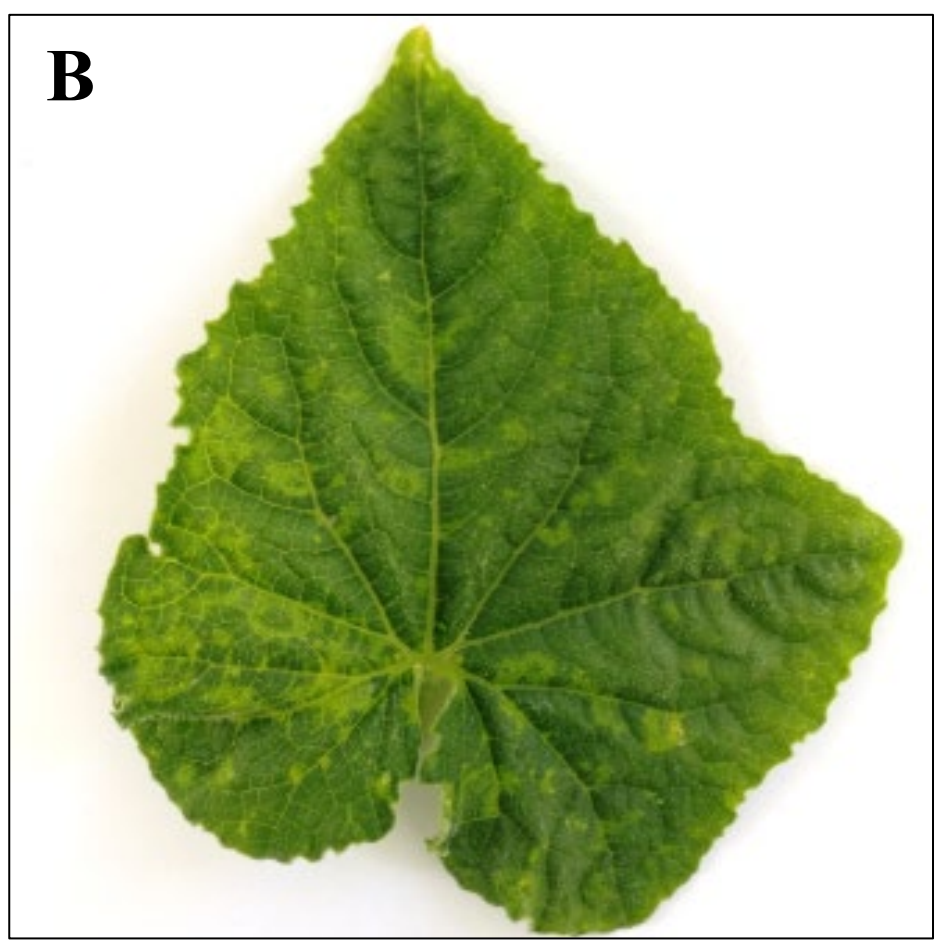
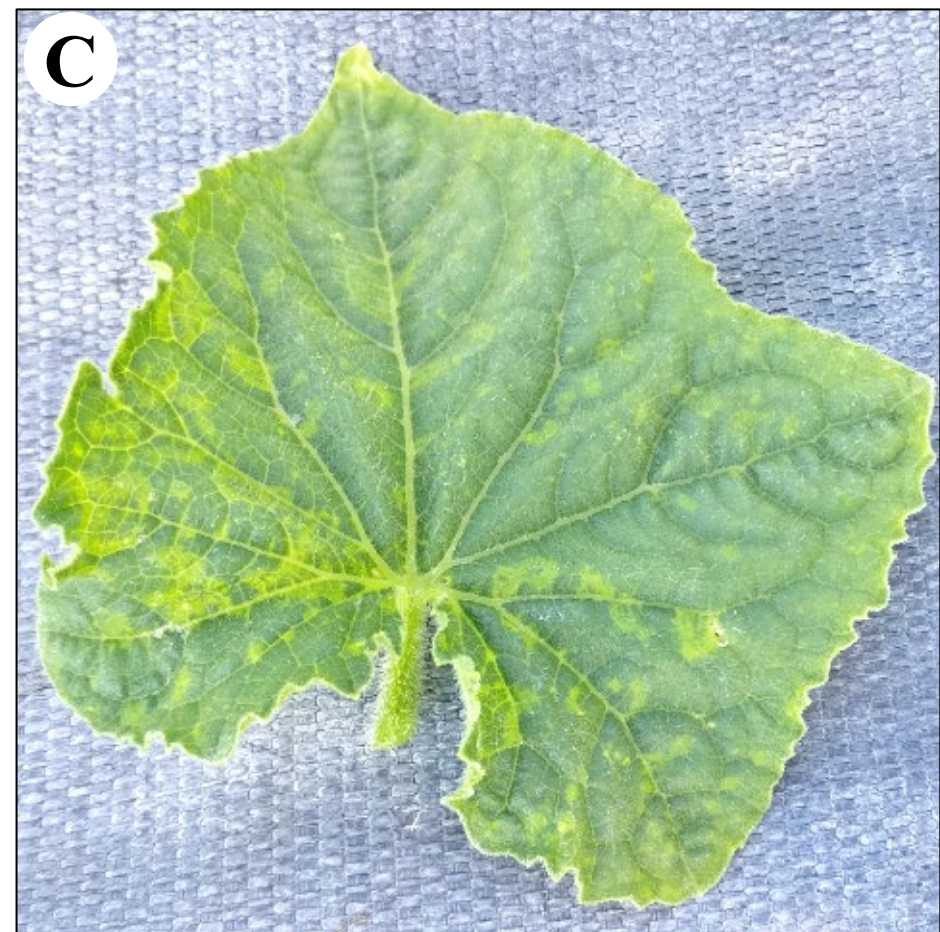




Clade I

Clade II

Figure 5



SUPPLEMENTARY INFORMATION

Table S1. Primers used for genome sequence completion of TRSV isolate WA-AM1.

Primer	Sequence (5' to 3')	Coordinates ^a	Purpose
A70	AGATTTCCAGAAGCTGGACGCC	1107-1128	TRSV RNA1 5'-RACE cDNA synthesis
A58	AGATGTGGCTTCAGATGCCT	861-880	TRSV RNA1 5'-RACE GSP1
A71	AATTGACACCATTGAAGGCGAT	674-695	TRSV RNA1 5'-RACE GSP2
A64	ATACCGAACAACTTCATGTTCAGTG	1055-1079	TRSV RNA2 5'-RACE cDNA synthesis
A65	AACCACTCTAAAGTTGTTGCGCACAAAG	617-644	TRSV RNA2 5'-RACE GSP1
A66	ATGTTGGCCAACAAAGTGAACAAT	362-386	TRSV RNA2 5'-RACE GSP2
A61	TTGGTAGCCCTGCTGGCATTAG	7058-7079	TRSV RNA1 3'-RACE GSP4
A62	TTAGTTTGCTGGCAACCATGT	7076-7096	TRSV RNA1 3'-RACE GSP5
A72	TTCCTGCCCTTACTAGGGTG	7159-7178	TRSV RNA1 3'-RACE GSP6
A67	TCAGGAGGGCAGTGTTTCCATC	3158-3179	TRSV RNA2 3'-RACE GSP4
A68	TGACTTGCGTCATACTGAAGCAGAG	3233-3257	TRSV RNA2 3'-RACE GSP5
A69	TAACCAGGATTGGTAGCCCTG	3462-3482	TRSV RNA2 3'-RACE GSP6
A73	TGGCGTCCAGCTTCTGGAAATCTG	1106-1129	TRSV RNA1 internal gap 1 completion
A75	TGCTATCCCTTCCACAGTAGGG	1462-1483	
A76	TTCATTATCCATGTAGACGCACGA	1639-1662	
A77	TGACTGTTTTGGCAATTTATTTGGCC	1573-1598	TRSV RNA1 internal gaps 2 and 3 completions
A78	TATCTTGGAGAAGACGCATGATTGCC	1663-1688	
A79	TACCCGCTTGGAATTTCCCAC	3238-3258	
A80	TTCTCTTTGAGTTGCAGTACTCTTGG	3495-3520	

A81	TTCTGGATCAAGTCCAGTTGCC	3829-3851	
A82	ATATGCTAGGCATCGTTTGGCTG	3883-3905	TRSV RNA1 internal gap 4 completion
A83	ATGCGTCCTTTCAAGCACATAGGG	4997-5020	
A84	ATCTCGAAGTTTCGAGTGCCAAG	5210-5232	
J114	GGTCTCGAGTTTTTTTTTTTTTTTTTT		Poly(T) reverse primer used in RT-PCRs for 3'- end sequence determination of TRSV RNA1 and RNA2

^aBased on TRSV isolate WA-AM1 genome segments (RNA1, MW495243 and RNA2, MW495244).

Table S2. Percent nucleotide sequence identity matrix of sequences corresponding to the D2-D3 expansion segment of the 28S LSU of *X. americanum* species group (*X. rivesi* isolate from this study indicated in bold font; PQ452334).

	1	2	3	4	5	6	7	8	9	10	11	12	13	14	15	16	17	18	19	20	21	22	23	24	25	26	27
1 PQ452334	ID																										
2 MK957230	99.98	ID																									
3 MK947997	99.99	99.97	ID																								
4 MK050001	99.99	99.99	99.99	ID																							
5 MH248816	99.98	99.99	99.98	99.99	ID																						
6 KX263157	99.99	99.98	99.99	99.98	99.98	ID																					
7 KX244909	99.80	99.80	99.81	99.81	99.80	99.80	ID																				
8 KX062682	99.79	99.79	99.79	99.79	99.79	99.79	99.98	ID																			
9 KU680968	99.99	99.97	99.99	99.98	99.98	100.00	99.80	99.79	ID																		
10 KU250156	99.82	99.82	99.82	99.82	99.82	99.83	99.81	99.80	99.83	ID																	
11 KP268963	99.84	99.84	99.84	99.84	99.84	99.84	99.84	99.83	99.84	99.85	ID																
12 KP268960	99.79	99.79	99.79	99.79	99.79	99.79	99.83	99.83	99.78	99.83	99.84	ID															
13 KJ802889	99.80	99.80	99.81	99.81	99.81	99.80	99.81	99.82	99.80	99.85	99.81	99.82	ID														
14 KF430800	99.99	99.99	99.99	100.00	99.99	99.98	99.81	99.79	99.98	99.82	99.84	99.79	99.81	ID													
15 JQ99004	99.98	99.99	99.98	99.99	99.98	99.98	99.80	99.79	99.98	99.82	99.83	99.78	99.80	99.99	ID												
16 JQ990036	99.81	99.80	99.81	99.81	99.81	99.81	99.95	99.95	99.80	99.81	99.85	99.82	99.81	99.81	99.80	ID											
17 HM163211	99.99	99.99	99.99	99.99	99.99	99.99	99.80	99.78	99.99	99.82	99.84	99.79	99.80	99.99	99.99	99.80	ID										
18 HM163210	99.97	99.97	99.96	99.98	99.98	99.96	99.79	99.78	99.96	99.82	99.82	99.78	99.80	99.98	99.97	99.79	99.97	ID									
19 DQ299511	99.99	99.97	99.99	99.98	99.98	99.99	99.80	99.79	99.99	99.83	99.83	99.78	99.80	99.98	99.98	99.80	99.98	99.97	ID								
20 DQ299507	99.99	99.97	99.99	99.98	99.98	99.99	99.80	99.79	99.99	99.83	99.83	99.78	99.80	99.98	99.98	99.80	99.98	99.97	100.00	ID							
21 DQ299504	99.98	99.97	99.99	99.98	99.97	99.99	99.80	99.79	99.99	99.82	99.83	99.78	99.80	99.98	99.98	99.80	99.98	99.97	99.98	99.98	ID						
22 DQ299495	99.99	99.97	99.99	99.98	99.98	99.99	99.80	99.79	100.00	99.82	99.84	99.78	99.80	99.98	99.98	99.80	99.99	99.96	99.98	99.99	99.99	ID					
23 AY601610	99.84	99.83	99.84	99.84	99.84	99.83	99.84	99.83	99.83	99.85	99.88	99.83	99.83	99.84	99.83	99.84	99.84	99.83	99.84	99.84	99.83	99.83	ID				
24 AY601603	99.98	99.98	99.98	99.99	99.99	99.98	99.80	99.78	99.98	99.81	99.83	99.78	99.81	99.99	99.98	99.80	99.99	99.98	99.97	99.98	99.98	99.98	99.84	ID			
25 AY601597	99.99	99.97	99.99	99.98	99.98	99.99	99.81	99.80	99.98	99.83	99.85	99.79	99.81	99.98	99.98	99.81	99.98	99.96	99.99	99.99	99.98	99.98	99.84	99.98	ID		

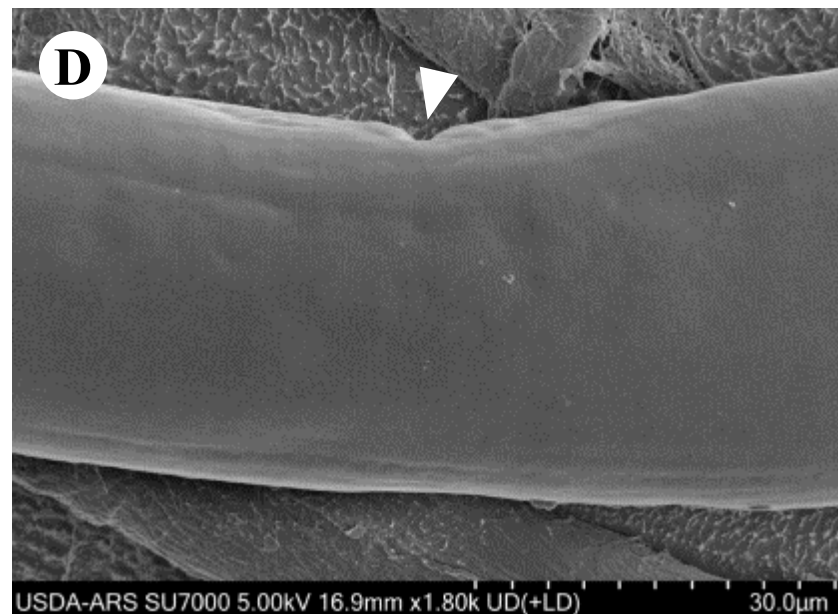
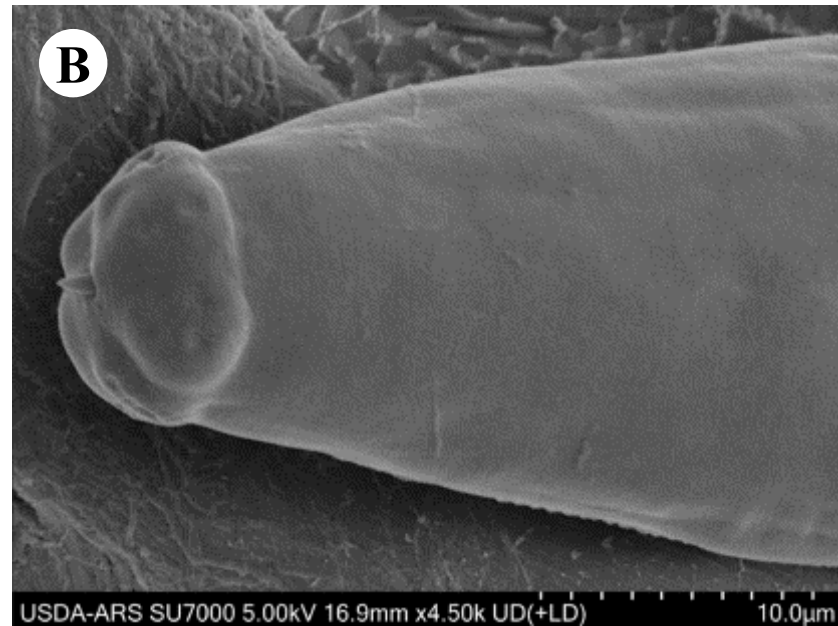
26 AY601596	99.99	99.97	99.99	99.98	99.98	99.99	99.80	99.79	99.99	99.83	99.84	99.79	99.80	99.98	99.98	99.81	99.98	99.96	99.99	99.99	99.98	99.98	99.84	99.98	100.00	ID	
27 AY601587	99.99	99.97	99.99	99.98	99.98	100.00	99.80	99.78	100.00	99.82	99.84	99.78	99.80	99.98	99.98	99.80	99.98	99.97	99.99	99.99	99.99	100.00	99.83	99.98	99.99	99.99	ID

MK957230: *X. himalayense* (Iran), MK947997: *X. oxycaudatum* (South Africa), MK050001: *X. diffusum* (South Korea), MH248816: *X. parataylori* (Slovakia), KX263157: *X. californicum* (CA, USA), KX244909: *X. incertum* (Spain), KX062682: *X. pachtaicum* (Tunisia), KU680968: *X. rivesi* (MD, USA), KU250156: *X. parasimile* (Bulgaria), KP268963: *X. duriense* (Spain), KP268960: *X. vallense* (Spain), KJ802889: *X. simile* (Greece), KF430800: *X. brevicollum* (Taiwan), JQ990042: *X. parabrevicolle* (Italy), JQ990036: *X. parapachydermum* (Spain), HM163211: *X. lambertii* (India), HM163210: *X. inaequale* (India), DQ299511: *X. tarjanense* (FL, USA), DQ299507: *X. floridae* (FL, USA), DQ299504: *X. laevistriatum* (FL, USA), DQ299495: *X. georgianum* (FL, USA), AY601610: *X. brevisicum* (Portugal), AY601603: *X. taylori* (Italy), AY601597: *X. incognitum* (PA, USA), AY601596: *X. bricolensis* (PA, USA), AY601587: *X. santos* (Portugal).

Table S3. Percent nucleotide sequence identity matrix of sequences corresponding to the ITS rRNA-coding region of *X. americanum* species group (*X. rivesi* isolate from this study indicated in bold font; PQ452333).

	1	2	3	4	5	6	7	8	9	10	11	12
1 PQ452333	ID											
2 HM990158	99.98	ID										
3 GQ231532	99.97	99.96	ID									
4 GQ231531	99.98	100.00	99.96	ID								
5 GQ231530	99.99	99.98	99.97	99.98	ID							
6 FR878063	99.99	99.98	99.97	99.98	99.99	ID						
7 DQ299536	99.97	99.95	99.95	99.96	99.97	99.97	ID					
8 DQ299532	99.96	99.95	99.95	99.96	99.97	99.96	99.99	ID				
9 DQ299519	99.98	99.97	99.96	99.97	99.98	99.98	99.96	99.96	ID			
10 AY580056	99.98	99.97	99.95	99.97	99.98	99.97	99.96	99.95	99.97	ID		
11 DQ299528	99.98	99.97	99.96	99.97	99.98	99.97	99.95	99.95	99.97	99.98	ID	
12 AY430176	99.99	99.98	99.97	99.98	100.00	99.99	99.97	99.96	99.98	99.98	99.98	ID

HM990158: *X. oxycaudatum* (Taiwan), GQ231532: *X. californicum* (Chile), GQ231531: *X. peruvianum* (Chile), GQ231530: *X. inaequale* (Chile), FR878063: *X. rivesi* (Italy), DQ299536: *X. tarjanense* (FL, USA), DQ299532: *X. floridae* (FL, USA), DQ299519: *X. citricolum* (FL, USA), AY580056: *X. americanum* (Belgium), DQ299528: *X. laevistriatum* (FL, USA), AY430176: *X. thornei* (Belgium).



Supplementary Figure S1. Low-Temperature Scanning Electron Microscopy (LT-SEM) images of *Xiphinema rivesi* adult females. A: entire adult female body, B: anterior end with lip region and slightly protruding stylet, C: tail region and posterior end, D: vulval region with vulva indicated by white arrowhead.